Multiple Thymic Cell Fate Decisions Regulated by Gads

Rose Shalah[*], Enas Hallumi[*], Naama Klopstock[*], Manal Marzouk[*] and Deborah Yablonski[*‖]

[*] Department of Immunology, Ruth and Bruce Rappaport Faculty of Medicine, Technion—Israel Institute of Technology, Haifa 3525433, Israel

[‖] Correspondence: Deborah Yablonski, +972-4-8295393 (Tel), debya@technion.ac.il

Abstract:

Gads is an immune adaptor that bridges the TCR-inducible interaction of two additional adaptors: SLP-76 and LAT. Thymic development is profoundly impaired in the absence of SLP-76 or LAT, but moderately impaired in Gads-deficient mice, which accumulate non-naïve ($CD44^+$) peripheral T cells. To better distinguish Gads-dependent and -independent developmental transitions, we performed tamoxifen-induced ablation of Gads ($Gads^{iKO}$), accompanied by the expression of tdTomato, and compared the co-development of Gads-expressing (Tom^-) and -ablated (Tom^+) thymocytes within the same mouse. The frequency of $Gads^{iKO}$ (Tom^+) thymocytes decreased at Gads-dependent junctures but remained high in Gads-independent lineages. Within the DN compartment, Gads was required for conventional β-selection, but not for the γδ or NKT lineages. $Gads^{iKO}$ DP thymocytes were overwhelmingly $CD5^-$, indicating impaired self peptide-MHC responsiveness; yet exhibited reduced death by neglect. Instead, an aberrant population of $CD5^-$ $Gads^{iKO}$ thymocytes progressed as far as the CD4 SP compartment, while lacking key characteristics of positively selected thymocytes. Distinct, $CD5^+$ $Gads^{iKO}$ SP populations were positively-selected and TCR responsive, suggesting that they include one or more Gads-independent developmental lineages. In particular, the development of innate-like NKT cells, $CD44^+$ $PLZF^+$ $CD4^+$ cells, and $CD44^+$ $Eomes^+$ $CD8^+$ cells was favored in the absence of Gads. Our results suggest that Gads regulates thymic development, by promoting conventional αβ T cell development and death by neglect, while suppressing innate-like thymic developmental fates.

Key points:

Gads is differentially required for conventional and innate-like thymic lineages

Gads is required to promote death by neglect in unselected DP thymocytes

Introduction

At every stage of their life cycle, T cell development, differentiation and function are tightly controlled by signaling through the clonotypic T cell antigen receptor (TCR). This principle is most clearly exemplified by thymocyte development, in which the strength of TCR signaling controls multiple developmental checkpoints [1-4].

Conventional thymocyte development proceeds through three main stages, known as double negative (DN, $CD4^-CD8^-$), double positive (DP, $CD4^+CD8^+$), and single positive (SP, either $CD4^+$ or $CD8^+$). The DN compartment may be further divided into four substages, based on the expression of surface markers, including DN1 ($CD44^+CD25^-$), DN2 ($CD44^+CD25^+$), DN3 ($CD44^-CD25^+$), and DN4 ($CD44^-CD25^-$) [5].

As thymocytes pass through the DN compartment, productive rearrangement of TCRβ is required for expression of the pre-TCR. Signals emanating from the pre-TCR trigger β-selection, which is characterized by rapid thymocyte proliferation, NF-κB activity, and upregulation of CD5, along with passage of DN3 thymocytes through DN4 and into the DP compartment [6-9].

The mature αβ TCR is first expressed during the DP stage, where its ability to recognize self peptide-MHC (p-MHC) can be assessed by following activation markers, such as increased expression of CD5 and surface TCRβ [9,10]. DP cells that fail to recognize self-p-MHC are removed through a process that has been denoted “death by neglect” [11,12]. On the other hand, strong recognition of self-p-MHC triggers death by negative selection. Between these two extremes, weak self-recognition triggers positive selection and transition to the SP compartments. Positively-selected SP cells are typically $TCR\beta^{hi}$ and $CD5^{hi}$, and follow a maturation trajectory, during which the expression of CCR7 transiently increases, CD24 decreases and CD62L increases, prior to their exit from the thymus as naive

(CD44^{lo}CD62L^{hi}) peripheral T cells. Taken together, the ability of T cells to correctly interpret the strength of TCR ligation profoundly shapes thymocyte development, eventually allowing T cells to distinguish between self and foreign antigens [1-4].

A number of smaller, non-conventional thymocyte populations typically develop in parallel to the above-described events. These include γδT cells, NKT cells, and a number of innate-like SP populations, which express characteristic transcription factors, such as PLZF or Eomes, as well as high expression of CD44 [13,14]. Evidence suggests that alterations in the strength or quality of TCR signaling may differentially affect the ability of thymocytes to progress through conventional vs non-conventional developmental pathways [14-16].

TCR ligation triggers a cascade of tyrosine kinases [17,18], initiated by a Src-family kinase, Lck, which activates a Syk-family kinase, ZAP-70. ZAP-70 phosphorylates two adaptor proteins, LAT and SLP-76 [19-25], triggering the SH2-mediated binding of multiple signaling proteins to the adaptors [reviewed in 26,27].

Gads is an evolutionarily conserved, Grb2-family adaptor, expressed mainly in T cells and mast cells, and required for optimal antigen receptor signaling in these cell types [28]. Like Grb2, Gads consists of a central SH2 domain flanked by two SH3 domains, but also includes a unique unstructured linker. Gads C-SH3 domain binds constitutively to SLP-76 [29-31], whereas its SH2 domain mediates the cooperative binding of Gads to two LAT phospho-sites, pY171 and pY191 [22,30,32]. Through these interactions, Gads bridges the TCR-induced recruitment of SLP-76 and its associated signaling proteins to phospho-LAT [33-37], where adaptor-associated enzymes trigger downstream responses [26,28,38]. Among the most important and best-understood downstream pathways, SLP-76-associated Itk phosphorylates LAT-associated PLC-γ1, triggering the production of second messengers that increase intracellular calcium.

Since the best understood function of Gads is to bridge the TCR-induced recruitment of SLP-76 to LAT, it is surprising that germline deletion of these adaptors results in distinct phenotypes. Both SLP-76 and LAT are essential for thymocyte development beyond the DN3 stage [39-41]. In contrast, Gads-deficient mice exhibit incomplete blocks at multiple thymic checkpoints, associated with a marked reduction in thymic size; nevertheless, the presence of prominent peripheral CD4 and CD8 T cell populations demonstrates that T cell development is at least partially Gads-independent [42,43]. To date, the precise thymic developmental transitions controlled by Gads are not fully understood. Germline deletion of Gads also results in the accumulation of non-naïve peripheral T cells [43]; however, the developmental origin of these cells is not known.

We hypothesized that Gads fine tunes TCR responsiveness and thymocyte development by exerting a mixture of positive and negative regulatory functions. Our hypothesis relates not only to the quantitative aspects of the TCR response, but also to qualitative aspects, such as the choice between alternative responses to TCR stimulation. To test our hypothesis, we established a new genetic model that enabled us to compare the development of Gads-expressing and Gads-ablated thymocytes, side by side in the same mouse.

This approach revealed multiple points at which Gads influences thymocyte development. Gads was required for efficient β-selection and for optimal p-MHC-induced expression of CD5, an important correlate of positive selection. On the other hand, Gads was required for efficient death by neglect of unselected thymocytes; in its absence, unselected, $CD5^-$ thymocytes progressed as far as the CD4 SP compartment. This observation sheds an unexpected light on the involvement of TCR signaling elements in the regulation of death by neglect. Remarkably, certain thymocyte lineages were able to develop in a Gads-independent manner. These included the γδ and NKT lineages, as well as certain $CD44^+$ innate-like SP lineages.

Materials and Methods

Antibodies and staining reagents

Anti-mouse antibodies CD4-PerCP-Cy5.5 or -FITC (Clone RM4-4 and GK1.5), CD8-APC-Cy7, or –APC, or –FITC (Clone 53-6.7 or QA17A07), CD44-BV421 (Clone IM7), CD5-BV711 (Clone 53-7.3), CD25-APC (Clone PC61), CD24-APC (Clone M1/69), CD62L-BV605 (Clone MEL-14), NK1.1-APC or -FITC (Clone PK136), TCR γδ-PerCP-Cy5.5 or -FITC (Clone GL3), TCR β-BV605 (Clone H57-597), CCR7-AF488 (Clone 4B12), EOMES-AF647 (Clone W17001A), Ly-6G/Ly-6C (Gr-1)-FITC (clone RB6-8C5), CD45R/B220-FITC (clone RA3-6B2), TER-119-FITC (clone TER-119), CD11b (Mac1)-Ly40-FITC (clone M1/70), Zombie Aqua Fixable viability kit, and Biotin-conjugated anti-mouse CD3ε (clone145-2C11), CD4 (clone RM4-4) and CD8 (clone 53-6.7) were from Biolegend. PLZF-AF488 (Clone Mags.21F7) was from Invitrogen eBioscience. Cleaved caspase 3-AF647 (Clone D3E9) was from Cell Signaling. Gads-AF647 (UW40) was from Santa Cruz Biotechnology. Unless noted otherwise, all PBS used in this study is without calcium and magnesium.

Mice

Mice were on the C57BL/6 background and maintained in an SPF facility under veterinary supervision and in accordance with institutional ethics guidelines. Gads-deficient ($Gads^{-/-}$) mice [42] were generously provided by C. Jane McGlade (University of Toronto). $Gads^{FL}$ mice, in which LoxP signals flank Grap2 (Gads) exon2, were generated for us by Cyagen/Taconic using a CRISPR/Cas9 approach. $Gads^{FL}$ mice were cross-bred to Jackson Laboratory strain #007914 (Ai14), to incorporate a Cre-dependent tdTomato ($Tom^{FL\text{-}stop}$) reporter at the Rosa26 locus [44]. The ubiquitously-expressed, tamoxifen-inducible UBC-Cre-ERT2 Cre recombinase [45] was maintained in a hemizygous state. To generate mice for

experiments, $Gads^{FL/FL}Tom^{FL\text{-}stop/FL\text{-}stop}$ mice were bred to Gads-deficient Cre driver mice ($Gads^{-/-}$UBC-Cre-ERT2^{+}), to generate $Gads^{FL/-}Tom^{FL\text{-}stop}$ progeny, either Cre^{+} or Cre^{-}.

Tamoxifen-inducible deletion of Gads

Tamoxifen (Sigma, T5648) was dissolved at 10 mg/ml in fresh corn oil by shaking at 37°C for 3-4 hr. For tamoxifen-inducible deletion of Gads, 6-7 week old $Gads^{FL/-}Tom^{FL\text{-}stop}$ mice, either UBC-Cre-ERT2^{+} or Cre^{-}, were treated with tamoxifen daily for five days by intraperitoneal injection (75 µg/g mouse weight). In this configuration, Cre-mediated recombination at a single allele of Gads and a single allele of tdTomato suffices to render the cells tdTomato-positive and Gads-deficient ($Tom^{+}Gads^{iKO}$).

Peripheral blood T cell phenotyping

To assess the efficiency of Cre-mediated recombination, 200 µl of blood was collected from the cheek into 1.5ml Eppendorf tubes containing 50 units heparin. Blood samples were diluted to 2ml in PBS and underlayed with 2 ml of Histopaque-1083 (Sigma, 10831). Following centrifugation at 400 g for 30 min at room temperature, leukocytes were collected from the interface, and washed once in PBS prior to staining for FACS analysis.

Thymocyte isolation and staining

A single cell suspension of thymocytes was generated by pressing the thymus through a 40 µm Cell Strainer. Cells were washed once with PBS supplemented with 2% FCS, then washed and re-suspended in 10 ml PBS without FCS. Cells were stained for 30 min at RT in the dark with Zombie Aqua Fixable Viability Kit. Staining was terminated by washing cells with 2ml FACS buffer (PBS, supplemented with 2% FCS and 0.02% sodium azide). Cells were then stained for 15-30 min at 4°C with a cocktail of fluorescently labeled antibodies in FACS buffer, washed once with FACS buffer and once with PBS, fixed for 20 min at RT in

the dark with a 1:1 dilution of fixation buffer in PBS (IC Fixation Buffer Thermo Fischer Scientific, 00-8222-49) or with Fixation buffer X1 (True-Nuclear Transcription Factor Buffer set, Biolegend, 424401), then washed in FACS buffer.

Intracellular staining

After fixation, cells were washed twice with permeabilization buffer. For intracellular staining with Gads, TCR or cleaved caspase 3, we used 1x Thermo Fischer Scientific permeabilization buffer (Invitrogen, 00-8333-56).For intracellular staining with PLZF and EOMES we used 1x True-Nuclear Transcription factor permeablization buffer (Biolegend, 424401). Cells were then stained for 30 min at RT with a cocktail of fluorescently labeled antibodies in the permeabilization buffer, and washed once with permeabilization buffer and once with FACS buffer.

Annexin V staining

After staining the cells with zombie and with the desired surface markers, cells were washed with Annexin V Binding Buffer (Biolegend, 422201). Cells were stained for 15 min at RT with annexin V (Biolegend, 640919), 10 ng/10^6, cells in annexin V binding buffer.

FACS analysis

Stained cells were read on a Fortessa II FACS analyzer, using single-stained cells or compensation beads as controls. Results were analyzed with FlowJo™ software, while gating on Zombie-negative singlet cells. Where indicated, a FITC-labeled dump gate was used to exclude NK1.1$^+$ and γδ$^+$ T cells, as well as cells that stained positive for Ly-6G/Ly-6C (Gr-1), CD45R/B220, TER-119, or CD11b (Mac1)-Ly40. In some cases, a modified dump gate was used to exclude cells staining with CD4, CD8, CD45R/B220, TER-119 or CD11b (Mac1)-Ly40, while including NK1.1$^+$ and γδ$^+$ T cells.

Calcium fluorimetry

Calcium flux was measured using a mixture of thymocytes from tamoxifen-treated Cre^+ and Cre^- mice. Five million thymocytes were washed with calcium staining buffer (RPMI supplemented with 1% FCS, 20mM Hepes PH 7.3, and 2mM Glutamine), and incubated in the dark in a 15 ml tube for 30 min at 30^0C, with 0.5 ml calcium staining buffer containing 4μM indo-1 AM (eBioscience, ratiometric intracellular calcium indicator), 2mM probenecid, fluorescent cell surface markers, including CD4-FITC (clone GK1.5) and CD8-APC (clone QA17A07), and 3μg/ml biotinylated stimulatory antibodies: CD3 alone, or with CD4 (clone RM4-4) and CD8 (clone 53-6.7). The stained cells were then washed twice and resuspended in calcium buffer RPMI, supplemented with 20mM Hepes PH 7.3 and 2mM Glutamine. Cells were stored on ice and preheated to 37^0C for 5 min prior to ratiometric calcium fluorimetry, which was performed by FACS, with the temperature maintained at 37 °C, and TCR stimulation was induced by adding 25 μg/ml streptavidin (Biolegend, 405150) at the 60 s time point. Excitation was at 355 nm and emission was measured using the bandpass filters 405/20 (Ca-bound indo-1) and 485/22 (free indo-1), with data presented as the ratio between these two values. Data analysis was performed on each subpopulation by gating on $CD5^+$, Tom^+ or Tom^- DP or SP thymocytes.

Statistical Analysis

All experiments in this study were performed two or more times, with similar results, with at least three mice from each genotype included in each experiment. Statistical analysis was performed using the Prism software package. p values were determined using the statistical tests indicated in figure legends. The following symbols were used to indicate statistically significant p values: *, $p<0.05$; **, $p<0.01$; ***, $p<0.0005$; ****, $p<0.0001$.

Results

A mouse model for inducible deletion of Gads, accompanied by the expression of tdTomato

To better distinguish Gads-dependent and -independent developmental pathways, we developed a mouse model system for the inducible deletion of Gads. This model is comprised of two "floxed" genes, $Gads^{FL}$ and $Tom^{FL\text{-}stop}$ (Fig 1A), controlled by a ubiquitously-expressed tamoxifen-inducible Cre recombinase, UBC-Cre-ERT2 [45]. Cre-mediated removal of Gads exon 2 creates a frameshift mutation that alters the protein sequence after K26, resulting in a premature stop codon after 29 amino acids (Fig 1B). $Tom^{FL\text{-}stop}$ is a previously-described fluorescent reporter, expression of which is blocked by a LoxP-flanked, upstream in-frame stop codon [44]. Cre-mediated removal of this stop cassette is required for expression of the tdTomato gene product. Together, this system permits Cre-mediated deletion of Gads, accompanied by the expression of tdTomato.

Prior to Cre-mediated ablation, $Gads^{FL}$ supports wild-type functionality

To validate our model, we first verified that, prior to its Cre-mediated ablation, $Gads^{FL}$ supports wild type functionality in the thymus, where Gads-deficient phenotypes are best-defined [28]. To this end, we compared thymic development in mice of three genotypes: $Gads^{+/-}$ (heterozygotes), $Gads^{FL/-}$ (in which one allele of Gads is floxed and the other is germ-line deleted), and $Gads^{-/-}$ (germ-line Gads-deficient mice).

As previously reported [42,43], $Gads^{-/-}$ mice had markedly reduced thymic cellularity (Supplemental Fig 1A), and exhibited a partial block at the DN to DP transition (Supplemental Fig 1B). This developmental block was reflected in an increased percentage of DN thymocytes, and reduced percentages of DP, CD4 SP, and CD8 SP thymocytes (Supplemental Fig 1C-F), accompanied by a reduced ratio of CD4 to CD8 SP thymocytes

(Supplemental Fig 1G). In all of these parameters, we observed statistically significant differences between Gads$^{-/-}$ and Gads$^{+/-}$ thymocytes, but no significant differences were observed between Gads$^{FL/-}$ and Gads$^{+/-}$ thymocytes (Supplemental Fig 1A and C-G).

Within the DN compartment, Gads$^{-/-}$ thymocytes exhibited the previously reported partial block at the DN3 to DN4 transition [42,43]. In this trait as well, Gads$^{-/-}$ DN thymocytes exhibited a statistically significant increase in the frequency of DN3 cells, which was not observed in Gads$^{FL/-}$ mice (Supplemental Fig 1H). These observations provide strong evidence that the LoxP sites surrounding Gads exon 2 do not impair the expression or function of Gads.

The tdTomato marker reliably identifies Gads^{iKO} peripheral T cells and thymocytes

Our typical experimental workflow is depicted in Fig 2A. For inducible deletion of Gads, we administer tamoxifen for five consecutive days to UBC-Cre-ERT2^{+} Gads$^{FL/-}$Tom$^{FL\text{-}stop}$ mice; in parallel, we tamoxifen-treat an equal number of control Cre^{-} Gads$^{FL/-}$Tom$^{FL\text{-}stop}$ litter-mates. We chose a genetic configuration in which one allele of Gads is germ-line disrupted and the other is floxed, so that Cre-mediated recombination at a single allele of Gads will suffice to render the cells Gads-deficient. In parallel, Cre-mediated recombination induces the expression of tdTomato (Tom).

Tom^{+} peripheral blood T cells were reproducibly observed one week after the initiation of tamoxifen treatment; however, their frequency varied between mice. The rapid appearance of Tom^{+} peripheral T cells suggests that they derive from Cre activity in pre-existing peripheral populations.

To more directly detect ablation of Gads, we stained PBLs intracellularly with a fluorescently-labeled anti-Gads antibody, and analyzed the results while gating on CD4^{+} or CD8^{+} T cells. Tom^{+} peripheral T cells were uniformly Gads-negative, (Fig 2B, top panels). A

tight correlation between the Tom$^+$ and Gads^{iKO} phenotypes was apparent as soon as one week after the initiation of tamoxifen treatment (Fig 2B, bottom panels) and remained intact as long as 5 weeks after the initiation of tamoxifen treatment (data not shown). Within the thymus, Tom$^+$ cells were likewise uniformly Gads-negative (Fig 2C). These results establish Tom$^+$ as a marker that reliably identifies Gads^{iKO} cells in our experimental system.

Thymocyte development begins in the DN quadrant, which is first populated by bone-marrow-derived common lymphoid progenitors [46]. Two weeks after the initiation of tamoxifen treatment, the frequency of Tom$^+$ DN thymocytes strongly resembled the frequency of Tom$^+$ PBLs in the same mouse (Fig 2D). This observation suggests that tamoxifen triggered UBC-Cre-ERT2-mediated recombination with comparable efficiency in thymic progenitor cells and in preexisting peripheral T cell compartments.

Cell-autonomous impairment of β-selection in Gads^{iKO} (Tom$^+$) thymocytes

The contemporaneous development of Tom$^+$ (Gads^{iKO}) and Tom$^-$ (Gads-expressing) thymocytes within the same mouse provided an opportunity to assess the cell-autonomous effects of Gads on thymocyte development.

To focus on conventional T cell development, we used a "dump" gate to exclude NK1.1$^+$ and TCRγδ$^+$ thymocytes as well as non-T lineage cells. We followed thymic progression within the dump^{neg} population, while gating separately on Gads-expressing (Tom$^-$) and Gads^{iKO} (Tom$^+$) thymocytes.

Tom$^+$ (Gads^{iKO}) thymocytes largely phenocopied the germline Gads-deficient mouse, exhibiting a partial block at the DN to DP transition compared to Cre$^-$ thymocytes (Fig 3A). This developmental block was reflected in a marked, statistically-significant increase in the frequency of DN thymocytes (Fig 3B) and reduced frequency of CD4 SP thymocytes (Fig 3C). The frequency of CD8 thymocytes was unchanged (Fig 3D) resulting in a reduced

CD4/CD8 ratio (Fig E). In contrast, Tom$^-$ thymocytes from the same Cre$^+$ mice closely resembled Cre$^-$ thymocytes (Fig 3A-E).

Within the DN compartment, Gads^{iKO} thymocytes exhibited a partial block at the DN3 to DN4 transition; in this trait as well Cre$^+$Tom$^-$ DN thymocytes phenocopied Cre$^-$ DN thymocytes, and both were statistically different from Gads^{iKO} DN thymocytes (Fig 3F).

We considered the possibility that selective impairment of Gads^{iKO} thymocytes may allow for compensatory progression of Tom$^-$ thymocytes, which would crowd out their Tom$^+$ counterparts. Since Gads-deficient mice are characterized by a small thymus [Supplemental Fig 1A and 42,43], we reasoned that cell-autonomous effects of Gads would result in a small thymus whereas compensatory progression of Tom$^-$ thymocytes may maintain normal thymic cellularity. Cellularity was rapidly and substantially reduced in tamoxifen-treated Cre$^+$ mice, relative to Cre$^-$ littermates (Fig 3G). This trend was most apparent in mice with the highest frequency of Tom$^+$ PBLs.

Taken together, our results suggest that the phenotypic effects of deleting Gads are predominantly cell-autonomous, with Tom$^-$ thymocytes largely following normal developmental pathways, while Tom$^+$ (Gads^{iKO}) thymocytes within the same mouse phenocopy germ-line Gads-deficient thymocytes.

These observations suggested a simple strategy to identify developmental junctions at which Gads exerts its effects. We posited that the frequency of Tom$^+$ thymocytes should decrease as cells pass through Gads-dependent developmental transitions. Conversely, the frequency of Tom$^+$ thymocytes may remain the same or even increase, in Gads-independent lineages. Consistent with the well-established partial blockage of Gads-deficient thymocytes at the β-selection and positive-selection checkpoints [42,43], the frequency of Tom$^+$ cells dropped substantially as cells passed from DN3 into DN4 (Fig 3H).

Conventional pre-TCR responsiveness depends on Gads

To better understand the mechanism by which Gads influences β-selection, we examined CD5, a marker for pre-TCR signaling, which, in turn, drives β-selection [9,47]. This analysis was conducted while using a dump gate to exclude non-conventional NK1.1^{+} and TCRγδ^{+} DN thymocytes.

TCRβ^{-}CD5^{-} DN2 cells represent a relatively early DN population (Fig. 4A, top row, pop. 1), that was used for normalization in this analysis. Within DN3, TCRβ expression was associated with moderate upregulation of CD5 in Gads-expressing thymocytes, but not in Gads^{iKO} thymocytes (Fig 4A, 2nd row). We refer to TCRβ^{+} DN3 cells that failed to upregulate CD5 or transit into DN4, as a population exhibiting arrested β-selection (Fig 4A, pop 2).

Among DN4 thymocytes, we observed an unusual population of Gads^{iKO} cells exhibiting impaired β-selection (Fig 4A, pop 3), as they remained CD5^{-} despite expressing TCRβ. In contrast, Gads-expressing, TCRβ^{+} DN4 thymocytes were uniformly CD5^{+}, suggesting that they represent a post β-selection population (Fig 4A, pop 4), composed thymocytes that have responded to pre-TCR signaling by passing the β-selection checkpoint.

To better define the juncture at which Gads affects conventional β-selection, we examined the frequency of Tom^{+} cells in each of the above populations of interest, relative to their frequency in the early DN population. The relative frequency of Tom^{+} cells increased in the arrested β-selection population, and markedly decreased in the CD5^{+}, post β-selection population (Fig 4B). Taken together, these results demonstrate that Gads is required for pre-TCR-induced expression of CD5, along with the associated progression from DN3 to DN4.

CD5 marks Gads-independent DN lineages

Despite markedly impaired β-selection (Fig 4A-B); thymocyte development persists in the absence of Gads [Fig 3 and 42,43]. This contradiction raised the possibility that certain

lineages may exhibit Gads-independent developmental progression. To search for such lineages in the DN compartment, we altered our gating strategy to include both conventional and non-conventional DN thymocytes, and characterized putatively signaling-competent cells by gating on populations of $CD5^+$ DN thymocytes (Fig 4C and 4D left panels).

This gating strategy revealed a population of $CD44^+CD5^+$ cells, which were predominantly $TCR\beta^+$ and $NK1.1^+$. This putative NKT population was detected both in Gads-expressing (Fig 4C, top right panel) and in $Gads^{iKO}$ DN thymocytes (Fig 4D, top right panel).

A distinct population of $CD44^-$ (DN3+4) $CD5^+$ cells included both conventional $TCR\beta^+$ and $TCR\gamma\delta^+$ thymocytes (Fig 4C and 4D, bottom right panels). Consistent with impaired β-selection, the $CD5^+TCR\beta^+$ population was more prominent in Gads-expressing thymocytes. In contrast, the $TCR\beta^-TCR\gamma\delta^+$ population predominated in $Gads^{iKO}$ DN thymocytes.

To more rigorously determine the dependence of each developmental pathway on Gads, we assessed the frequency of Tom^+ cells in each lineage, while normalizing to the frequency of Tom^+ cells found in an early DN1+2 ($CD44^+CD5^-$) DN population from the same mouse. The relative frequency of Tom^+ thymocytes was markedly decreased in conventional $CD5^+$ DN cells ($TCR\beta^+NK1.1^-$) but was not significantly changed in the $CD5^+TCR\gamma\delta^+$ population, nor was it significantly changed in the $CD5^+NK1.1^+$ population (Fig 4E).

Our results provide strong evidence that Gads is differentially required for different T cell lineages. In particular, Gads is selectively required for conventional β-selection, but not for the development of γδ or NKT DN thymocytes. Moreover, the vast majority of NKT and γδ DN thymocytes were CD5-positive, even among $Gads^{iKO}$ DN thymocytes (data not shown). This CD5-positivity strongly suggests that particular thymocyte lineages may be capable of Gads-independent TCR signaling.

Gads promotes TCR responsiveness, while also facilitating death by neglect

In conventional T cell development, β-selection is followed by progression to the DP compartment. DP thymocytes are then tested for TCR-mediated recognition of self-peptide-MHC antigens, which induces further upregulation of CD5 and TCRβ.

In line with previous studies [10,48], we estimated TCR-driven progression through the DP compartment by subdividing it into unselected ($CD5^{-}$), low responders ($CD5^{med}TCR\beta^{med}$) and high responders ($CD5^{hi}TCR\beta^{hi}$) (Fig 5A). $Gads^{iKO}$ (Tom^{+}) DP thymocytes were significantly more likely to be unselected and less likely to be low or high responders (Fig 5 A and B). Indeed, a prominent, $CD5^{-}$ $Gads^{iKO}$ DP population was observed at all time points that we examined from 2-6.5 weeks after the initiation of tamoxifen treatment (data not shown). The DP subset distribution was similarly skewed in germ-line Gads-deficient mice (Supplemental Fig 2A-B), suggesting that an unselected DP phenotype is a core characteristic of Gads-deficient thymocyte development.

TCR expression, as detected by intracellular staining with TCRβ, was comparable in $Gads^{iKO}$ and Gads-expressing DP thymocytes (Fig 5C). We therefore attribute the predominantly unselected phenotype of $Gads^{iKO}$ DP thymocytes to a TCR signaling defect.

To further verify a TCR signaling defect, we measured TCR-induced calcium flux, using an *ex vivo*, FACS-based assay. In brief, a mixture of Tom^{+} and Tom^{-} thymocytes was fluorescently stained with anti-CD4, -CD8 and -CD5, along with biotinylated stimulatory antibodies, and stimulation was induced by the addition of streptavidin. As a control for cell viability and intact calcium stores, ionomycin-induced calcium flux was not affected by Gads (data not shown).

After measuring baseline calcium at 37°C, cells were triggered by streptavidin-mediated co-cross-linking of CD3, CD4 and CD8, to mimic co-receptor-dependent recognition of MHC.

CD5$^-$ DP cells did not increase calcium in this assay (data not shown); we therefore analyzed the data while gating on a CD5$^+$ DP population, defined in Supplemental Fig 3A. This gate produced well-matched surface TCRβ expression in Tom$^+$ and Tom$^-$ cells (Supplemental Fig 3B left). Moreover, intracellular staining verified that Tom$^+$ DP cells within the CD5$^+$ gate were indeed Gads- deficient (Supplemental Fig 3B right).

Upon TCR stimulation, intracellular calcium increased in Gads-expressing (Tom$^-$) DP thymocytes, but this response was blunted in Gads^{iKO} DP thymocytes (Fig 5D); when analyzed on a single-cell basis, the frequency of responding CD5$^+$ DP thymocytes was reduced 6.8-fold in the absence of Gads (Fig 5E). These data confirm a profound signaling defect in Gads-deficient DP thymocytes, even within the CD5$^+$, potentially responsive gate.

Peptide-MHC-non-responsive, unselected DP thymocytes are candidates for death by neglect [12], a multi-step, apoptotic process, in which cleavage-mediated activation of caspase 3 is followed by surface exposure of phosphatidyl serine, which can be measured by staining with annexin V. The marked accumulation of unselected Gads^{iKO} DP thymocytes raised the question of whether Gads may influence the process of death by neglect.

The average frequency of cleaved caspase 3$^+$ cells within the unselected DP gate was slightly reduced in the absence of Gads (Fig 5F), but this difference was not statistically significant, due to wide inter-mouse variation (data not shown). However, a statistically significant trend was observed upon pairwise comparison of Tom$^+$ and Tom$^-$ unselected DP thymocytes within the same mouse (Fig 5G). Further downstream, the frequency of annexin V$^+$ unselected DP cells was substantially and significantly reduced in the absence of Gads (Fig 5H and 5I).

Taken together, our data suggest two ways in which Gads regulates progression through the DP compartment. First, Gads is required for optimal responsiveness of DP thymocytes to

self-peptide-MHC, as evidenced by the failure of Gads^{iKO} DP thymocytes to upregulate CD5 *in vivo*, and by their markedly reduced TCR responsiveness *ex vivo*. Second, Gads is required to promote death by neglect in unselected, CD5^{-} DP thymocytes. These twin defects likely explain the accumulation of unselected, CD5^{-} Gads^{iKO} DP thymocytes.

Parallel progression of selected and unselected Gads^{iKO} thymocytes into the CD4 SP compartment

Despite the poor TCR-responsiveness of Gads^{iKO} DP thymocytes (see Fig 5D), Gads-deficient thymocytes progressed to the SP populations (see Fig 3A and Supplemental Fig 1B), raising the question of whether passage of Gads-deficient thymocytes into the SP compartments is driven by positive selection. To address this question, we examined well-known surface markers of positive selection among SP thymocytes: increased expression of CD5, TCRβ, and CCR7, along with decreased expression of CD24 [49,50]. To exclude any potential non-SP populations from this analysis, we used "tight" SP gates, as illustrated in Fig 3A.

Consistent with positive selection, the vast majority of Gads-expressing CD4 SP thymocytes were found within a TCRβ^{hi}CD5^{hi} gate. (Fig 6A, left panels). Moreover, most Gads^{iKO} (Tom^{+}) CD4 SP thymocytes were found within the TCRβ^{hi}CD5^{hi} gate (Fig 6A, right panel). Finally, nearly all CD8 SP thymocytes, whether Gads-expressing or Gads^{iKO} were found within the TCRβ^{hi}CD5^{hi} gate (Supplemental Fig 4A).

Additional markers provided further support for the existence of positively-selected Gads^{iKO} SP populations. Whether Gads-expressing or Gads^{iKO}, CD5^{+} CD4 SP thymocytes were found on a trajectory of increasing CCR7 and decreasing CD24, as compared to the DP population from which they derived (Fig 6B). These markers suggest that, despite low TCR-

responsiveness in the DP compartment, a subset of Gads^{iKO} thymocytes may undergo TCR-driven positive selection.

To further verify TCR-responsiveness of CD5^{+} Gads^{iKO} SP populations, we measured TCR-induced calcium flux, in a mixture of Tom^{+} and Tom^{-} thymocytes, while gating on the CD5^{+}, CD4 and CD8 SP populations. Within the CD5^{+} expression gate used for this assay, TCR expression was somewhat lower in the Gads^{iKO} (Tom^{+}) CD4 SP population (Supplemental Fig 3C left panel) but was well matched with Gads-expressing cells in the CD8 SP population (Supplemental Fig 3D left panel). Moreover, we verified by intracellular staining that CD5^{+}Tom^{+} CD4 and CD8 SP thymocytes were indeed Gads-deficient (Supplemental Figs 3C and D right panels).

To achieve different intensities of TCR stimulation, we stimulated the cells by crosslinking CD3 alone, or together with the CD4 or CD8 co-receptors. Upon co-cross-linking CD3 and CD4, increased calcium was observed, both in Gads-expressing and in Gads^{iKO} CD5^{+} CD4 SP thymocytes (Fig 6C, top panels). Nevertheless, both the amplitude of the response and the frequency of responding cells were reduced in the absence of Gads (Fig 6C, top panels and Fig 6D). The signaling defect of Gads^{iKO} CD4 SP thymocytes was more pronounced when the thymocytes were stimulated via cross-linking of CD3 alone (Fig 6C, bottom panels and 6E).

TCR-induced calcium flux was likewise observed in CD5^{+} CD8 SP thymocytes, upon co-cross-linking of CD3 and CD8; and in this case it was not reduced in the absence of Gads (Supplemental Fig 4B, top panels and Supplemental Fig 4C). A moderate reduction of calcium flux was observed in Gads^{iKO} CD8 SP thymocytes, when they were stimulated by co-cross-linking CD3 alone (Supplemental Fig 4B, bottom panels and Supplemental Fig 4D). Taken together, we conclude that a prominent subset of Gads^{iKO} SP thymocytes derive from positive selection and are capable of TCR responsiveness.

A distinct population of Gads^{iKO} CD4 SP thymocytes was found in an unusual TCRβ^{lo}CD5^{-} population (Fig 6A, right panel), that was nearly absent in Gads-expressing cells (Fig 6F). Whereas Tom^{-} cells predominated in the DP and positively-selected SP populations, the TCRβ^{lo}CD5^{-} population was composed almost entirely of Tom^{+} cells (Fig 6G). This TCRβ^{lo}CD5^{-} Gads^{iKO} CD4 SP population was observed at all time points that we examined from 2-6.5 weeks after the initiation of tamoxifen treatment (data not shown). A similar TCRβ^{lo}CD5^{-} CD4 SP population was found in germline Gads-deficient mice (Supplemental Fig 2C). Both the prevalence and the absolute number of TCRβ^{lo}CD5^{-} CD4 SP thymocytes were markedly increased in germline Gads-deficient mice as compared to age-matched wild type mice (Supplemental Fig 2D), Together, these results suggest that the TCRβ^{lo}CD5^{-} CD4 SP population is an atypical population that is a conserved feature of Gads-deficient thymocyte development.

The TCRβ^{lo}CD5^{-} CD4 SP population was clearly part of the T cell lineage, as demonstrated by its strong intracellular staining with TCRβ (Fig 6H). Nevertheless, cells in this population did not exhibit signs of positive selection. In addition to low expression of CD5, CD24 expression remained high and CCR7 remained low (Fig 6I). Together, these data suggest that thymocytes within the TCRβ^{lo}CD5^{-} CD4 SP population passed into the CD4 SP compartment without undergoing positive selection.

Taken together, our data suggest two potential pathways of CD4 SP development in the absence of Gads. On the one hand CD5^{+} Gads^{iKO} SP thymocytes exhibit TCR responsiveness and appear to result from positive selection. On the other hand, CD5^{-} Gads^{iKO} appear to develop in the absence of positive selection; these thymocytes may derive from unselected DP thymocytes that did not undergo death by neglect; rather progressing as far as the CD4 SP compartment. We speculate that progression of this population into the SP compartment may be driven by the cytokine milieu. Consistent with this notion, a substantial proportion of

the $CD5^-$ $Gads^{iKO}$ CD4 SP thymocytes were $CD25^+$ (Fig 6J). We do not have any evidence that this population exits the thymus, and believe it may be a "dead end" thymic population that accumulates in the absence of Gads.

Altered maturation of positively-selected $Gads^{iKO}$ SP thymocytes

The presence of TCR-responsive, $CD5^+$ $Gads^{iKO}$ SP thymocytes demonstrated that Gads is not universally-required for positive selection. To better understand the nature of positively-selected $Gads^{iKO}$ thymocytes, we further characterized the $CD5^+$ SP populations.

Based on accepted markers [49], we subdivided $CD5^+$ SP thymocytes into immature ($CD24^{hi}CD62L^{med}$), mature ($CD24^-CD62L^{hi}$), and an additional $CD24^-CD62L^{lo}$ population (Fig 7A and 7B). In the absence of Gads, the frequency of immature CD4 SP thymocytes decreased, whereas mature CD4 thymocytes moderately increased, and the $CD24^-CD62L^{lo}$ population was markedly increased (Fig 7C, left panels). Similarly, the frequency of immature CD8 SP thymocytes markedly decreased in the absence of Gads whereas mature CD8 SP thymocytes increased (7C, right panels). The CD8 compartment did not include a substantial $CD24^-CD62L^{lo}$ population, either in the presence or in the absence of Gads.

We considered the possibility that population frequencies may be skewed by the small size of the Tom^+ SP populations. To more rigorously determine how Gads affects progression within the SP compartments, we compared the frequency of Tom^+ cells in each sub-compartment. Relative to the DP compartment, the frequency of Tom^+ cells was markedly decreased in the immature CD4 and CD8 SP populations, and significantly increased in the $CD24^-CD62L^{lo}$ CD4 SP population (Fig 7D). These observations suggest that cell fate decisions within the SP compartments are substantially altered in the absence of Gads.

The $CD24^-CD62L^{lo}$ CD4 SP population was $TCR\beta^+$ and included a prominent population of $NK1.1^+$ cells (Fig 7E); moreover, a high proportion of $CD24^-CD62L^{lo}$ cells expressed PLZF

(Fig 7F), a transcription factor expressed in certain innate-like thymic lineages [13]. These observations first suggested to us that the $CD24^{-}CD62L^{lo}$ population may be enriched for innate-like CD4 SP thymocyte lineages, whose development may be Gads-independent.

Gads-independent development of innate-like SP lineages

To better determine whether Gads may regulate the development of innate-like thymic SP lineages, we measured additional markers of innate-like thymocytes.

Within the CD4 SP compartment, we observed a $CD44^{hi}CD62L^{lo}$ population (Fig 8A) whose frequency was profoundly increased in the absence of Gads (Fig 8B). $CD44^{hi}$ CD4 SP thymocytes tended to express PLZF (Fig 8C), a marker of innate-like CD4 thymic lineages. Within the CD8 SP compartment, $CD44^{hi}$ thymocytes tended to express Eomes (Fig 8D), a marker of innate-like CD8 SP lineages.

The frequency of $CD44^{hi}PLZF^{+}$ CD4 SP thymocytes profoundly increased in the absence of Gads (Fig 8E); moreover, the frequency of $CD44^{hi}$ $Eomes^{+}$ CD8 SP thymocytes was moderately but significantly increased in the absence of Gads (Fig 8F). Taken together, these results suggest that the development of innate-like thymic lineages may be favored in the absence of Gads. To more rigorously test this notion, we examined the frequency of Tom^{+} cells in the innate-like compartments. When compared to the DP compartment, the frequency of Tom^{+} cells was significantly increased within the $CD44^{hi}PLZF^{+}$ CD4 SP and the $CD44^{hi}Eomes^{+}$ CD8 SP populations (Fig 8G). These data provide strong evidence that Gads is dispensable for the development of innate-like thymic lineages; and even suggest the possibility that these lineages may be favored in the absence of Gads.

Discussion

Despite years of research, the precise regulatory roles of Gads in thymic development remain unclear. To illuminate this issue, we developed a mouse model in which Gads-expressing and Gads-ablated thymocytes develop side by side in the same animal. Ablation was driven by a ubiquitously-expressed, tamoxifen inducible Cre recombinase, with tamoxifen administered 2.5-3.5 weeks prior to harvesting thymi. Thus, the $Gads^{iKO}$ thymic populations that we analyzed were largely derived from progenitor cells that underwent ablation of Gads prior to entering the thymus. In this model, Gads-ablated thymocytes exhibited largely cell autonomous phenotypes that resembled germline Gads-deficient thymocytes, whereas Gads-expressing thymocytes in the same mouse phenocopied wild type thymocytes.

The co-development of Gads-expressing (Tom^-) and Gads-ablated (Tom^+) thymocytes allowed us to more rigorously identify developmental transitions at which Gads plays a role. Within the DN compartment, Gads was required for efficient β-selection, and for the consequent pre-TCR-induced increase in the expression of CD5. Yet ablation of Gads did not perturb the development of $CD5^+$ γδ thymocytes and NKT cells within the DN compartment. This result first suggested to us that Gads may be selectively required for particular thymocyte lineages. A similar pattern was seen in the SP compartments, where $CD5^+$ Gads-deficient thymocytes tended towards non-conventional, innate-like lineages.

Our results are consistent with the β-selection defect previously observed in germline Gads-deficient mice [42,43], and with the failure of Gads-deficient DN thymocytes to respond to anti-CD3 stimulation [42]. To gain further insight into this phenomenon, we developed an approach to assess physiologic pre-TCR signaling *in vivo*, based on the established relationship between pre-TCR signaling and CD5 expression [9]. Our approach revealed that substantial populations of $Gads^{iKO}$ DN thymocytes fail to upregulate CD5 or progress to DN4

despite expressing surface TCR-β. Among Gads^{iKO} cells that transited to DN4, cells with low to medium TCRβ expression failed to upregulate CD5 which was expressed only on DN4 thymocytes with the highest expression of TCRβ. These findings provide strong confirmation that the developmental defects of Gads-deficient DN thymocytes can be connected to a pre-TCR signaling defect.

Likewise, substantial evidence suggests that Gads is required in the DP compartment to support signaling through the mature αβ TCR. Previous studies demonstrated that Gads-deficient, TCR-transgenic mice have prominent defects in positive and negative selection [42,51]. We extended these studies to a polyclonal TCR repertoire by using CD5 as a physiologic marker that correlates with TCR signaling intensity *in vivo* [9]. In both the inducible and the germline-deleted mouse model, most Gads-deficient DP thymocytes failed to upregulate CD5, indicating impaired responsiveness to self-MHC. Moreover, even CD5^{+} Gads^{iKO} DP thymocytes exhibited profoundly reduced TCR-induced calcium influx. Together, these results suggest a profound TCR-signaling defect in Gads-deficient DP.

The TCR signaling defect likely reflects the role of Gads in mediating the TCR-induced recruitment of SLP-76 to LAT. This task is facilitated by the high affinity (low nanomolar) constitutive binding of Gads to SLP-76 [29]. Grb2 most likely cannot compensate for Gads, since its binding to SLP-76 occurs at 1000-fold lower affinity [29]. Thus, TCR-induced recruitment of SLP-76 to LAT is profoundly reduced in the absence of Gads, but is not affected by deletion of other Grb2-family members [36,52].

Given the reduced TCR signaling competence of Gads-deficient DP thymocytes, one might expect to see increased death by neglect, which occurs in MHC-non-responsive wild-type thymocytes [11,12]. Yet the striking accumulation of CD5^{-} annexin V^{-} Gads^{iKO} DP thymocytes suggests that Gads is required for optimal death by neglect in unselected DP

thymocytes. Perhaps consistent with an involvement of Gads in cell death, Gads contains a caspase 3 cleavage site [53,54]; moreover, Gads-deficient T1 B cells were shown to be resistant to BCR-induced apoptosis [55]. Alternatively, our observations may suggest that in the absence of Gads, TCR signaling is reduced to a level that is sufficient for survival but insufficient for positive selection.

Surprisingly, unselected, $CD5^-$ thymocytes progressed as far as the CD4 compartment, where they remained in an immature, $CD24^{hi}TCR\beta^{lo}CCR7^{lo}$ state. This population likely corresponds to the $CD24^{hi}TCR\beta^{lo}$ transitional CD4 SP population that accumulates in TCR-transgenic Gads-deficient mice [51]. A population of $CD24^{hi}$ CD8 SP thymocyes was likewise observed in cyclososporin-treated HY-transgenic female mice [56]. Together, these results suggest that upon partial disruption of TCR signaling, unselected thymocytes may advance to the SP compartments, but fail to fully mature. Whereas Dalheimer *et al.* interpreted their results as an indication of uncoupling of positive selection from developmental progression [51], we suggest that the developmental progression of unselected Gads-deficient thymocytes may reflect a failure of death by neglect.

In parallel, we observed distinct populations of $CD5^+$, apparently signaling-competent, Gads-deficient thymocytes. The Gads-deficient $CD5^+$ populations include DN NKT cells, DN γδ thymocytes, and positively-selected $CD5^+$ SP thymocytes. Gads-independent developmental progression of $CD5^+$ populations suggests the possibility of Gads-independent TCR responsiveness. Consistent with this notion, several lines of evidence suggest that Gads is not essential for TCR responsiveness, but rather appears to regulate the probability of response to low intensity TCR signals [36,43,57]. Residual Gads-independent TCR responsiveness may be sufficient to support the development of particular non-canonical populations, which may favor populations that require only low-level TCR signaling for their development. Moreover, the delicate balance between positive and negative regulators of TCR

responsiveness may be altered in innate-like populations, in a way that permits Gads-independent TCR responsiveness.

The γδ thymocyte population is an example of a population that does not require strong TCR signaling for its progression, as the development of γδ DN thymocytes was not impaired in cyclosporine-treated mice [58]. In a previous study, germ-line deletion of Gads profoundly decreased TCRβ^+ DN4 cells but only moderately decreased the number of TCR$\gamma\delta^+$ DN4 cells per thymus [59]. The moderate decrease in γδ DN thymocytes may be related to the overall thymic atrophy of germline Gads-deficient mice. Our approach of comparing Gads-expressing and -ablated cells within the same thymus better controls for differences between mice, and therefore provides stronger evidence that Gads is not required for the development of γδ DN thymocytes.

In the SP compartments, we observed preferential development of innate-like lineages in the absence of Gads. Among CD8 SP thymocytes we observed a prominent population of positively-selected CD5$^+$ Gads^{iKO} innate-like cells that were CD44^{hi} and Eomes$^+$. Further supporting our observations, about half of the CD8 SP thymocytes from germline Gads-deficient mice were previously shown to express CD122, a marker of innate-like CD8 thymocytes [51]. Within the CD4 SP compartment, we observed a prominent population of positively-selected Gads^{iKO} CD4 SP thymocytes that were PLZF$^+$ and CD24$^-$, as well as CD62L^{lo} and CD44^{hi}, suggesting an activated phenotype. Many of these innate-like CD4 SP cells were NK1.1$^+$, suggesting that they may represent NKT cells. Relative to the DP population as a whole, the innate-like CD4 and CD8 SP populations were relatively enriched for Tom$^+$ cells. This result provides quantitative evidence for preferential developmental progression of Gads-deficient thymocytes into innate-like thymocyte subsets.

Previous research suggests that partial impairment of the TCR signaling pathway can markedly change the balance between conventional and innate-like thymocyte development. For example, mutation of SLP-76 Y145, one of the Itk binding-sites on SLP-76 [60], promotes preferential development of CD44^{hi} CD122^{+} Eomes^{+} innate-like CD8 thymocytes [14]. Development of innate-like CD4 and CD8 SP thymocytes was also markedly favored in the absence of Itk, but was abolished in the absence of SAP [15,16,61,62]. We extend this paradigm by providing evidence that, similar to the effect of Itk, the development of innate-like CD4 and CD8 SP thymocytes is favored in the absence of Gads.

One important difference between Gads and Itk is their effect on NKT cell development. Whereas both Itk and SAP are required to promote the development of CD4 SP NKT thymocytes [15,16,63,64], NKT development was not perturbed in the absence of Gads.

Previous studies have shown that non-naive, CD44^{hi} peripheral T cells predominate in germline Gads-deficient mice [43]. Such non-naive cells may be a product of altered thymic development, as was previously seen upon impairment of Itk signaling [14,15,65]. Alternatively, reduced thymic output in germline Gads-deficient mice may trigger lymphopenic expansion of peripheral T cells, with concomitant acquisition of an activated or memory phenotype, as is seen even in developmentally-normal T cells [66]. Finally, partial disruption of the TCR signaling pathway may impair post-thymic homeostasis, even in the absence of lymphopenia [see for example 67,68,69].

Our results are consistent with the possibility that, in the absence of Gads, innate-like, apparently non-naive cells are preferentially produced by the thymus, likely resulting in their predominance in the periphery. This interpretation suggests that, in future studies, it will be important to revisit the peripheral regulatory functions of Gads in developmentally normal T cells.

Acknowledgements: Pamela Schwartzberg and Dominic Golec from the NIH/NIAID and Leslie Berg from the University of Colorado provided much appreciated input into the interpretation of thymic phenotypes. The Biomedical Core Facility (BCF) of the Rappaport Faculty of Medicine provided access to FACS equipment, and BCF staff members Ofer Shenker, Amir Grau and Rotem Honen Kadosh provided excellent technical support. Gads-deficient mice were generously provided by C. Jane McGlade (University of Toronto). We thank our chief veterinarians Dr. Rona Shofti and Dr Dvir Mintz, as well as Paul Zannou, and the rest of the excellent staff from the Technion Preclinical Authority for professional assistance with the care, treatment and housing of the mice.

References

1. Morris, G.P., and P.M. Allen. 2012. How the TCR balances sensitivity and specificity for the recognition of self and pathogens. *Nat Immunol* 13:121-128.
2. Moran, A.E., and K.A. Hogquist. 2012. T-cell receptor affinity in thymic development. *Immunology* 135:261-267.
3. Fu, G., V. Rybakin, J. Brzostek, W. Paster, O. Acuto, and N.R.J. Gascoigne. 2014. Fine-tuning T cell receptor signaling to control T cell development. *Trends in Immunology* 35:311-318.
4. Hogquist, K.A., and S.C. Jameson. 2014. The self-obsession of T cells: how TCR signaling thresholds affect fate 'decisions' and effector function. *Nat Immunol* 15:815-823.
5. Godfrey, D.I., J. Kennedy, T. Suda, and A. Zlotnik. 1993. A developmental pathway involving four phenotypically and functionally distinct subsets of CD3-CD4-CD8-triple-negative adult mouse thymocytes defined by CD44 and CD25 expression. *The Journal of Immunology* 150:4244-4252.
6. Aifantis, I., M. Mandal, K. Sawai, A. Ferrando, and T. Vilimas. 2006. Regulation of T-cell progenitor survival and cell-cycle entry by the pre-T-cell receptor. *Immunological Reviews* 209:159-169.
7. Voll, R.E., E. Jimi, R.J. Phillips, D.F. Barber, M. Rincon, A.C. Hayday, R.A. Flavell, and S. Ghosh. 2000. NF-κB Activation by the Pre-T Cell Receptor Serves as a Selective Survival Signal in T Lymphocyte Development. *Immunity* 13:677-689.
8. Aifantis, I., F. Gounari, L. Scorrano, C. Borowski, and H. von Boehmer. 2001. Constitutive pre-TCR signaling promotes differentiation through Ca2+ mobilization and activation of NF-kappaB and NFAT. *Nat Immunol* 2:403-409.

9. Azzam, H.S., A. Grinberg, K. Lui, H. Shen, E.W. Shores, and P.E. Love. 1998. CD5 Expression Is Developmentally Regulated By T Cell Receptor (TCR) Signals and TCR Avidity. *Journal of Experimental Medicine* 188:2301-2311.

10. Breed, E.R., M. Watanabe, and K.A. Hogquist. 2019. Measuring Thymic Clonal Deletion at the Population Level. *J Immunol* 202:3226-3233.

11. Surh, C.D., and J. Sprent. 1994. T-cell apoptosis detected in situ during positive and negative selection in the thymus. *Nature* 372:100-103.

12. Szondy, Z., É. Garabuczi, K. Tóth, B. Kiss, and K. Köröskényi. 2012. Thymocyte death by neglect: Contribution of engulfing macrophages. *European Journal of Immunology* 42:1662-1667.

13. Pellicci, D.G., H.F. Koay, and S.P. Berzins. 2020. Thymic development of unconventional T cells: how NKT cells, MAIT cells and gammadelta T cells emerge. *Nat Rev Immunol* 20:756-770.

14. Gordon, S.M., S.A. Carty, J.S. Kim, T. Zou, J. Smith-Garvin, E.S. Alonzo, E. Haimm, D.B. Sant'Angelo, G.A. Koretzky, S.L. Reiner, and M.S. Jordan. 2011. Requirements for eomesodermin and promyelocytic leukemia zinc finger in the development of innate-like CD8+ T cells. *J Immunol* 186:4573-4578.

15. Prince, A.L., L.B. Watkin, C.C. Yin, L.K. Selin, J. Kang, P.L. Schwartzberg, and L.J. Berg. 2014. Innate PLZF^{+}CD4^{+} αβ T Cells Develop and Expand in the Absence of Itk. *The Journal of Immunology* 193:673-687.

16. Prince, A.L., Z. Kraus, S.A. Carty, C. Ng, C.C. Yin, M.S. Jordan, P.L. Schwartzberg, and L.J. Berg. 2014. Development of Innate CD4^{+} and CD8^{+} T Cells in Itk-Deficient Mice Is Regulated by Distinct Pathways. *The Journal of Immunology* 193:688-699.

17. Brownlie, R.J., and R. Zamoyska. 2013. T cell receptor signalling networks: branched, diversified and bounded. *Nat Rev Immunol* 13:257-269.

18. Chakraborty, A.K., and A. Weiss. 2014. Insights into the initiation of TCR signaling. *Nat Immunol* 15:798-807.

19. Lin, J., and A. Weiss. 2001. Identification of the minimal tyrosine residues required for linker for activation of T cell function. *J. Biol. Chem.* 276:29588-29595.

20. Paz, P.E., S. Wang, H. Clarke, X. Lu, D. Stokoe, and A. Abo. 2001. Mapping the Zap-70 phosphorylation sites on LAT (linker for activation of T cells) required for recruitment and activation of signalling proteins in T cells. *Biochem J* 356:461-471.

21. Zhang, W., R.P. Trible, M. Zhu, S.K. Liu, C.J. McGlade, and L.E. Samelson. 2000. Association of Grb2, Gads and Phospholipase C-g1 with phosphorylated LAT tyrosine residues. *J. Biol. Chem.* 275:23355-23361.

22. Zhu, M., E. Janssen, and W. Zhang. 2003. Minimal requirement of tyrosine residues of linker for activation of T cells in TCR signaling and thymocyte development. *J Immunol* 170:325-333.

23. Wardenburg, J.B., C. Fu, J.K. Jackman, H. Flotow, S.E. Wilkinson, D.H. Williams, R. Johnson, G. Kong, A.C. Chan, and P.R. Findell. 1996. Phosphorylation of SLP-76 by the ZAP-70 protein-tyrosine kinase is required for T-cell receptor function. *J. Biol. Chem.* 271:19641-19644.

24. Fang, N., D.G. Motto, S.E. Ross, and G.A. Koretzky. 1996. Tyrosines 113, 128, and 145 of SLP-76 are required for optimal augmentation of NFAT promoter activity. *J. Immunol.* 157:3769-3773.

25. Sela, M., Y. Bogin, D. Beach, T. Oellerich, J. Lehne, J.E. Smith-Garvin, M. Okumura, E. Starosvetsky, R. Kosoff, E. Libman, G. Koretzky, T. Kambayashi, H. Urlaub, J. Wienands, J. Chernoff, and D. Yablonski. 2011. Sequential phosphorylation of SLP-76 at tyrosine 173 is required for activation of T and mast cells. *The EMBO journal* 30:3160-3172.

26. Balagopalan, L., N.P. Coussens, E. Sherman, L.E. Samelson, and C.L. Sommers. 2010. The LAT Story: A Tale of Cooperativity, Coordination, and Choreography. *Cold Spring Harbor Perspectives in Biology* 2:a00 5512.

27. Koretzky, G.A., F. Abtahian, and M.A. Silverman. 2006. SLP76 and SLP65: complex regulation of signalling in lymphocytes and beyond. *Nat. Rev. Immunol.* 6:67-78.

28. Yablonski, D. 2019. Bridging the Gap: Modulatory Roles of the Grb2-Family Adaptor, Gads, in Cellular and Allergic Immune Responses. *Frontiers in Immunology* 10:doi: 10.3389/fimmu.2019.01704.

29. Seet, B.T., D.M. Berry, J.S. Maltzman, J. Shabason, M. Raina, G.A. Koretzky, C.J. McGlade, and T. Pawson. 2007. Efficient T-cell receptor signaling requires a high-affinity interaction between the Gads C-SH3 domain and the SLP-76 RxxK motif. *The EMBO journal* 26:678-689.

30. Houtman, J.C., Y. Higashimoto, N. Dimasi, S. Cho, H. Yamaguchi, B. Bowden, C. Regan, E.L. Malchiodi, R. Mariuzza, P. Schuck, E. Appella, and L.E. Samelson. 2004. Binding specificity of multiprotein signaling complexes is determined by both cooperative interactions and affinity preferences. *Biochemistry* 43:4170-4178.

31. Liu, Q., D. Berry, P. Nash, T. Pawson, C.J. McGlade, and S.S. Li. 2003. Structural basis for specific binding of the Gads SH3 domain to an RxxK motif-containing SLP-76 peptide: a novel mode of peptide recognition. *Mol Cell* 11:471-481.

32. Sukenik, S., M.P. Frushicheva, C. Waknin-Lellouche, E. Hallumi, T. Ifrach, R. Shalah, D. Beach, R. Avidan, I. Oz, E. Libman, A. Aronheim, O. Lewinson, and D. Yablonski. 2017. Dimerization of the adaptor Gads facilitates antigen receptor signaling by promoting the cooperative binding of Gads to the adaptor LAT. *Sci Signal* 10:eaal1482.

33. Asada, H., N. Ishii, Y. Sasaki, K. Endo, H. Kasai, N. Tanaka, T. Takeshita, S. Tsuchiya, T. Konno, and K. Sugamura. 1999. Grf40, a novel Grb2 family member, is

involved in T cell signaling through interactions with SLP-76 and LAT. *J. Exp. Med* 189:1383-1390.

34. Law, C.-L., M.K. Ewings, P.M. Chaudhary, S.A. Solow, T.J. Yun, A.J. Marshall, L. Hood, and E.A. Clark. 1999. GrpL, a Grb2-related adaptor protein, interacts with SLP-76 to regulate Nuclear Factor of Activated T Cell activation. *J. Exp. Med* 189:1243-1253.

35. Liu, S.K., N. Fang, G.A. Koretzky, and C.J. McGlade. 1999. The hematopoietic-specific adaptor protein Gads functions in T-cell signaling via interactions with the SLP-76 and LAT adaptors. *Curr. Biol.* 9:67-75.

36. Lugassy, J., J. Corso, D. Beach, T. Petrik, T. Oellerich, H. Urlaub, and D. Yablonski. 2015. Modulation of TCR responsiveness by the Grb2-family adaptor, Gads. *Cell Signal* 27:125-134.

37. Bilal, M.Y., E.Y. Zhang, B. Dinkel, D. Hardy, T.M. Yankee, and J.C. Houtman. 2015. GADS is required for TCR-mediated calcium influx and cytokine release, but not cellular adhesion, in human T cells. *Cell Signal* 27:841-850.

38. Jordan, M.S., and G.A. Koretzky. 2010. Coordination of receptor signaling in multiple hematopoietic cell lineages by the adaptor protein SLP-76. *Cold Spring Harb Perspect Biol* 2:a002501.

39. Clements, J.L., B. Yang, S.E. Ross-Barta, S.L. Eliason, R.F. Hrstka, R.A. Williamson, and G.A. Koretzky. 1998. Requirement for the leukocyte-specific adapter protein SLP-76 for normal T cell development. *Science* 281:416-419.

40. Pivniouk, V., E. Tsitsikov, P. Swinton, G. Rathbun, F.W. Alt, and R.S. Geha. 1998. Impaired viability and profound block in thymocyte development in mice lacking the adaptor protein SLP-76. *Cell* 94:229-238.

41. Zhang, W., C.L. Sommers, D.N. Burshtyn, C.C. Stebbins, J.B. DeJarnette, R.P. Trible, A. Grinberg, H.C. Tsay, H.M. Jacobs, C.M. Kessler, E.O. Long, P.E. Love, and L.E. Samelson. 1999. Essential role of LAT in T cell development. *Immunity* 10:323-332.

42. Yoder, J., C. Pham, Y.-M. Iizuka, O. Kanagawa, S.K. Liu, J. McGlade, and A.M. Cheng. 2001. Requirement for the SLP-76 adaptor GADS in T cell development. *Science* 291:1987-1991.

43. Yankee, T.M., T.J. Yun, K.E. Draves, K. Ganesh, M.J. Bevan, K. Murali-Krishna, and E.A. Clark. 2004. The Gads (GrpL) adaptor protein regulates T cell homeostasis. *J Immunol* 173:1711-1720.

44. Madisen, L., T.A. Zwingman, S.M. Sunkin, S.W. Oh, H.A. Zariwala, H. Gu, L.L. Ng, R.D. Palmiter, M.J. Hawrylycz, A.R. Jones, E.S. Lein, and H. Zeng. 2010. A robust and high-throughput Cre reporting and characterization system for the whole mouse brain. *Nature Neuroscience* 13:133-140.

45. Ruzankina, Y., C. Pinzon-Guzman, A. Asare, T. Ong, L. Pontano, G. Cotsarelis, V.P. Zediak, M. Velez, A. Bhandoola, and E.J. Brown. 2007. Deletion of the Developmentally Essential Gene *ATR* in Adult Mice Leads to Age-Related Phenotypes and Stem Cell Loss. *Cell Stem Cell* 1:113-126.

46. Shortman, K., and L. Wu. 1996. Early T lymphocyte progenitors. *Annu Rev Immunol* 14:29-47.

47. Hoffman, E.S., L. Passoni, T. Crompton, T.M. Leu, D.G. Schatz, A. Koff, M.J. Owen, and A.C. Hayday. 1996. Productive T-cell receptor beta-chain gene rearrangement: coincident regulation of cell cycle and clonality during development in vivo. *Genes Dev* 10:948-962.

48. Saini, M., C. Sinclair, D. Marshall, M. Tolaini, S. Sakaguchi, and B. Seddon. 2010. Regulation of *Zap70* Expression During Thymocyte Development Enables Temporal

Separation of CD4 and CD8 Repertoire Selection at Different Signaling Thresholds. *Science Signaling* 3:ra23-ra23.

49. Weinreich, M.A., and K.A. Hogquist. 2008. Thymic emigration: when and how T cells leave home. *J Immunol* 181:2265-2270.

50. Witt, C.M., and E.A. Robey. 2004. The ins and outs of CCR7 in the thymus. *J Exp Med* 200:405-409.

51. Dalheimer, S.L., L. Zeng, K.E. Draves, A. Hassaballa, N.N. Jiwa, T.D. Parrish, E.A. Clark, and T.M. Yankee. 2009. Gads-deficient thymocytes are blocked at the transitional single positive CD4+ stage. *Eur J Immunol* 39:1395-1404.

52. Ruminski, K., J. Celis-Gutierrez, N. Jarmuzynski, E. Maturin, S. Audebert, M. Malissen, L. Camoin, G. Voisinne, B. Malissen, and R. Roncagalli. 2023. Mapping the SLP76 interactome in T cells lacking each of the GRB2-family adaptors reveals molecular plasticity of the TCR signaling pathway. *Front Immunol* 14:1139123.

53. Berry, D.M., S.J. Benn, A.M. Cheng, and C.J. McGlade. 2001. Caspase-dependent cleavage of the hematopoietic specific adaptor protein Gads alters signalling from the T cell receptor. *Oncogene* 20:1203-1211.

54. Yankee, T.M., K.E. Draves, M.K. Ewings, E.A. Clark, and J.D. Graves. 2001. CD95/Fas induces cleavage of the GrpL/Gads adaptor and desensitization of antigen receptor signaling. *Proc Natl Acad Sci U S A* 98:6789-6793.

55. Yankee, T.M., K.E. Draves, and E.A. Clark. 2005. Expression and function of the adaptor protein Gads in murine B cells. *Eur J Immunol* 35:1184-1192.

56. Urdahl, K.B., D.M. Pardoll, and M.K. Jenkins. 1994. Cyclosporin A inhibits positive selection and delays negative selection in alpha beta TCR transgenic mice. *J Immunol* 152:2853-2859.

57. Zhang, E.Y., B.L. Parker, and T.M. Yankee. 2011. Gads Regulates the Expansion Phase of CD8+ T Cell-Mediated Immunity. *The Journal of Immunology* 186:4579-4589.

58. Jenkins, M.K., R.H. Schwartz, and D.M. Pardoll. 1988. Effects of cyclosporine A on T cell development and clonal deletion. *Science* 241:1655-1658.

59. Zeng, L., S.L. Dalheimer, and T.M. Yankee. 2007. Gads-/- mice reveal functionally distinct subsets of TCRbeta+ CD4-CD8- double-negative thymocytes. *J Immunol* 179:1013-1021.

60. Bunnell, S.C., M. Diehn, M.B. Yaffe, P.R. Findell, L.C. Cantley, and L.J. Berg. 2000. Biochemical interactions integrating Itk with the T Cell Receptor-initiated signaling cascade. *J. Biol. Chem.* 275:2219-2230.

61. Atherly, L.O., J.A. Lucas, M. Felices, C.C. Yin, S.L. Reiner, and L.J. Berg. 2006. The Tec Family Tyrosine Kinases Itk and Rlk Regulate the Development of Conventional CD8+ T Cells. *Immunity* 25:79-91.

62. Hu, J., and A. August. 2008. Naïve and Innate Memory Phenotype $CD4^+$ T Cells Have Different Requirements for Active Itk for Their Development. *The Journal of Immunology* 180:6544-6552.

63. Gerth, E., and J. Mattner. 2019. The Role of Adaptor Proteins in the Biology of Natural Killer T (NKT) Cells. *Front Immunol* 10:1449.

64. Felices, M., and L.J. Berg. 2008. The Tec kinases Itk and Rlk regulate NKT cell maturation, cytokine production, and survival. *J Immunol* 180:3007-3018.

65. Prince, A.L., C.C. Yin, M.E. Enos, M. Felices, and L.J. Berg. 2009. The Tec kinases Itk and Rlk regulate conventional versus innate T-cell development. *Immunological Reviews* 228:115-131.

66. Jameson, S.C. 2002. Maintaining the norm: T-cell homeostasis. *Nat Rev Immunol* 2:547-556.

67. Sonnenberg, G.F., P.R. Mangan, N.A. Bezman, D.R. Sekiguchi, E.T. Luning Prak, J. Erikson, J.S. Maltzman, M.S. Jordan, and G.A. Koretzky. 2010. Mislocalization of SLP-76 leads to aberrant inflammatory cytokine and autoantibody production. *Blood* 115:2186-2195.

68. Shen, S., M.I. Chuck, M. Zhu, D.M. Fuller, C.W. Yang, and W. Zhang. 2010. The importance of LAT in the activation, homeostasis, and regulatory function of T cells. *J Biol Chem* 285:35393-35405.

69. Yamada, K., M. Zuka, K. Ito, K. Mizuguchi, Y. Kakuchi, T. Onoe, Y. Suzuki, M. Yamagishi, S. Izui, M. Malissen, B. Malissen, and M. Kawano. 2018. LatY136F knock-in mouse model for human IgG4-related disease. *PLoS One* 13:e0198417.

Footnotes

Funding: This research was supported by grants to DY from the Israel Science Foundation (283/22), the Rappaport Family Institute for Research in the Medical Sciences, the Minerva Center on Cell Intelligence and the Colleck Research Fund.

Conflicts of Interest: The authors declare no conflict of interest. The funders had no role in the design of the study; in the collection, analyses, or interpretation of data; in the writing of the manuscript, or in the decision to publish the results.

Author contributions: RS and DY developed the study objectives and experimental strategy with key inputs from EH and MM. RS, EH and MM performed experiments, analyzed data and prepared the figures. NK designed and carried out all breeding and genotyping strategies for these experiments. This manuscript was written by DY and RS. All authors have read and agreed to the published version of the manuscript.

Supplemental Figures are attached to this submission as a separate PDF file.

Figure Legends

Fig 1. A mouse model for inducible deletion of Gads. The Gads^{iKO} mouse model comprises two "floxed" genes, whose expression is controlled by UBC-Cre-ERT2, a ubiquitously expressed tamoxifen-inducible Cre recombinase [45]. (**A**) Prior to Cre activity, LoxP sites flank exon 2 of Grap2, the gene that encodes Gads. Within the Rosa26 locus, a second set of LoxP sites flank an in frame stop codon that prevents the expression of a fluorescent marker, tdTomato [44]. (**B**) Cre-mediated recombination removes exon 2 of Grap2, creating a frameshift mutation that alters the protein sequence after K26 and results in a premature stop codon after 29 amino acids.

Fig 2. Tamoxifen-induced deletion of Gads is accompanied by the expression of tdTomato. (**A**) Experimental workflow for tamoxifen-inducible ablation of Gads. Created with BioRender.com. (**B**) One week after starting tamoxifen treatment, peripheral blood leukocytes (PBL) were stained for surface markers and intracellularly for Gads. Top: representative results obtained while gating on CD4$^+$ or CD8$^+$ T cells. Bottom: The frequency of Gads$^+$ and Tom$^+$ phenotypes observed in the CD4$^+$ and CD8$^+$ peripheral blood populations of 13 individual Cre$^+$ mice. The Pearson correlation coefficient (r) was calculated using Prism. (**C**) Two weeks after the start of tamoxifen, thymocytes were stained intracellularly for Gads. Representative result is presented while gating on live thymocytes. (**D**) Two weeks after the start of tamoxifen, total thymocytes were stained to identify DN (CD4$^-$CD8$^-$) cells. The frequency of Tom$^+$ DN thymocytes correlated with the frequency of Tom$^+$ PBLs observed four days earlier in the same mice.

Fig 3. Cell autonomous developmental phenotypes of Gads^{iKO} thymocytes. Mice were tamoxifen treated as in Fig 2A, and thymi were collected 2.5 weeks after starting tamoxifen. (**A-F and H**) Thymic developmental markers were assessed by FACS using cohorts of mice

in which 60-80% of Cre^+ PBLs were Tom^+. Zombie staining was used to exclude dead thymocytes. A mixture of FITC labeled antibodies was used to create a "dump gate" to exclude $NK1.1^+$ and $TCR\gamma\delta^+$ thymocytes, as well as erythrocyte, granulocyte, macrophage, monocyte and B cell lineages, as described in Methods. (**A**) Representative distribution of CD4 and CD8 surface markers within the live, $dump^{neg}$ population, assessed while gating separately on Tom^- ($Gads^{FL/-}$) and Tom^+ ($Gads^{iKO}$) thymocytes. (**B-D**) The percent of thymocytes found within each of the subpopulations defined in A. (**E**) The ratio of CD4 SP to CD8 SP thymocytes. (**F**) Progression through the DN substages was assessed while gating separately on live, $dump^{neg}$ Tom^+ and Tom^- DN ($CD4^-CD8^-$) thymocytes. Left: Representative result. Right: Quantitation of the results using the gating strategy shown at left. The legend relates to bar graphs B-F: Cre^- ($Gads^{FL/-}$), open bars; Cre^+Tom^- ($Gads^{FL/-}$), grey bars; Cre^+Tom^+ ($Gads^{iKO}$), striped bars. n = 8 Cre^- and 6 Cre^+ mice; data are cumulative from 3 cohorts of mice analyzed using the same protocol. Error bars indicate the standard deviation. Statistical significance was determined by a one-way ANOVA test, Tukey's multiple comparison test. (**G**) Reduced thymic cellularity in $Gads^{iKO}$ mice. Total thymic cellularity is plotted as a function of the frequency of Tom^+ PBLs. Cre^- mice are plotted on the Y axis. A linear regression confirmed a tendency to reduced thymus size with increased frequency of Tom^+ cells. To increase the number of data points, this panel combines data from multiple experiments in which thymi were collected 1.5-2.5 weeks after starting tamoxifen. n= 13 Cre^- and 14 Cre^+ mice. (**H**) The percent of Tom^+ thymocytes was determined while gating separately on each of the indicated sub-populations. To facilitate statistically valid comparisons between mice, the frequency of Tom^+ cells in each sub-stage was normalized to their frequency in the DN1 compartment of the same mouse. (n=6 Cre^+ mice from three cohorts). Statistical significance was determined by a one-way ANOVA test, Dunnett's multiple comparisons test.

Fig 4. Gads controls developmental decisions within the DN compartment. Thymocytes from Fig 3 were further analyzed by FACS 2.5 weeks after the initiation of tamoxifen treatment. (**A-B**) Analysis was performed while gating on live, dump^{neg} Tom^{+} and Tom^{-} DN substages, as defined in Fig 3F. (**A**) Representative distribution of TCRβ and CD5 expression within each DN compartment. Subpopulations of interest are indicated by numbers and defined in the table at right. (**B**) The percent of Tom^{+} cells within each of the DN subpopulations defined in A was normalized to the percent of Tom^{+} cells in the early DN (DN2 TCRβ^{-} CD5^{-}) compartment of the same mouse (n = 6 Cre^{+} mice). (**C-E**) DN thymocytes were analyzed using a modified dump gate that does not exclude NK or γδ T cells (n= 3 mice of each genotype). (**C**) Representative distribution of CD44 and CD5 surface markers within the DN compartment of a Cre^{-} mouse. Arrows indicate the strategy used to define CD5^{+} subpopulations of interest. (**D**) Tom^{+} Gads^{iKO} DN subpopulations were analyzed using the gating strategy shown in C. (**E**) The percent of Tom^{+} cells within each of the DN subpopulations defined in D was normalized to the percent of Tom^{+} cells in the DN1+2 CD5^{-} compartment of the same mouse (n= 3 Cre^{+} mice). Error bars indicate the standard deviation. Statistical significance was determined by one-way ANOVA, Dunnett's multiple comparisons test, Dunnett's multiple comparisons test (**B and E**).

Fig 5. Gads promotes TCR responsiveness, while also facilitating death by neglect. 2-2.5 weeks after the initiation of tamoxifen treatment, thymocytes were analyzed by FACS while gating on the live DP (CD4^{+}CD8^{+}) population, defined as in Fig 3A. (**A**) Expression of CD5 and TCRβ was detected using surface staining. Representative result. DP subpopulations are defined at right. (**B**) The percent of DP cells within each of the DP subpopulations defined in A. Statistical significance was determined by a one-way ANOVA Tukey's multiple comparison test. (**C**) TCRβ was detected by intracellular staining. (**D-E**) TCR-induced calcium flux. Tom^{+} and Tom^{-} thymocytes were mixed together and stained with the calcium

indicator, indo-1, fluorescent cell surface markers, and biotinylated stimulatory antibodies (CD3, CD4 and CD8). Calcium fluorimetry was performed by FACS at 37°C, with stimulation initiated at the 60 sec time point by the addition of streptavidin. The indo-1 ratio is shown as a function of time, while gating on $CD5^+$, Tom^+ or Tom^-, DP thymocytes. (**D**) Representative result. The double headed arrow marks an ~50 sec time window within which we calculated the percent of responding cells. (**E**) The percent of cells exhibiting an indo-1 ratio >1 within the time window shown in D. n=3 repeats. Error bars were too small to depict. Statistical significance was determined by unpaired T-test. (**F**) cleaved caspase 3 was detected by intracellular staining while gating on the unselected DP population, as defined in A. (**G**) Paired comparison of the percent of cleaved caspase 3^+ cells, observed within the Tom^+ and Tom^- unselected DP populations from 8 individual Cre^+ mice. Statistical significance was determined by paired T-test. (**H**) Annexin V staining was analyzed while gating on the unselected DP population. (**I**) The frequency of annexin V^+ cells observed within the unselected DP populations. n=8 Cre^- and 7 Cre^+ mice. Statistical significance was determined by a one-way ANOVA Tukey's multiple comparison test.

Fig 6. Parallel progression of selected and unselected $Gads^{iKO}$ thymocytes into the CD4 SP compartment. 2.5 weeks after the initiation of tamoxifen treatment (or 2 weeks in the case of the calcium experiment) thymocytes were analyzed by FACS while gating on the live $CD4^+$ SP population, defined as in Fig 3A. (**A**) Expression of CD5 and TCRβ was detected using surface staining. Representative result. (**B**) Expression of CCR7 and CD24 was detected using surface staining while gating on the indicated $CD5^+$ DP and CD4 SP populations. Representative result. (**C-E**) TCR-induced calcium flux was analyzed as described in Fig 5D-E., but while gating on the $CD5^+$ CD4 SP population. (**F-G**) Quantitative analysis of the experiment shown in A. (**F**) The frequency of $CD5^-$ $TCR\beta^{lo}$ thymocytes within the CD4 SP population. Statistical significance was determined by one-way ANOVA

Tukey's multiple comparisons test. n=4 mice of each genotype (**G**) The percent of Tom$^+$ thymocytes within each of the indicated gates. Statistical significance was determined by one-way ANOVA Dunnett's multiple comparisons test. n= 4 Cre$^+$ mice. (**H**) Expression of Intracellular TCRβ and CD5 in Gads^{iKO} CD4 SP thymocytes. (I) Expression of CD24 and CCR7 was detected as in B, but while gating on the CD5$^-$ Gads^{iKO} DP and CD4 SP populations. (**J**) CD25 was detected by extracellular staining while gating on the indicated populations.

Fig 7. Altered maturation of positively-selected Gads^{iKO} SP thymocytes. 3.5-4 weeks after the initiation of tamoxifen treatment, thymocytes were analyzed by FACS while gating on the live, CD5$^+$, CD4$^+$ and CD8$^+$ SP populations, which were defined as in Fig 3A. n= 3 Cre$^-$ and 4 Cre$^+$ mice (**A and B**) Representative surface expression of CD24 and CD62L. (**C**) Frequency of immature (CD24^{hi}CD62L^{med}), mature (CD24$^-$CD62L^{hi}) and CD24$^-$CD62L^{lo} thymocytes within the CD5$^+$ SP populations. Statistical significance was determined by a one-way ANOVA Tukey's multiple comparisons test. (**D**) The frequency of Tom$^+$ cells within each of the maturation stages defined in A and B was compared to the DP population (n= 4 Cre$^+$ mice). Statistical significance was determined by a one-way ANOVA Dunnett's multiple comparisons test. (**E**) Representative expression of TCRβ and NK1.1 was assessed within the CD24$^-$CD62L^{lo} CD4 SP population. **(F)** Intracellular expression of PLZF in Tom$^-$ and Tom$^+$ within the CD24$^-$CD62L^{lo} CD4 SP population.

Fig 8. Gads-independent development of innate-like SP lineages. 2.5 weeks after the initiation of tamoxifen treatment, thymocytes were analyzed by FACS while gating on the live, CD5$^+$, CD4$^+$ and CD8$^+$ SP populations, defined as in Fig 3A. n= 8 Cre$^-$ and 7 Cre$^+$ mice (**A**) Representative surface expression of CD44 and CD62L. (**B**) Frequency of the CD44^{hi} CD62L^{lo} population, as defined in A. (**C**) Representative surface expression of CD44 and

PLZF in the $CD5^{+}CD4$ SP population. (**D**) Representative expression of CD44 and Eomes in the $CD5^{+}CD8$ SP population. (**E-F**) Frequency of $CD44^{hi}$ $PLZF^{+}$ among CD4 SP cells and $CD44^{hi}$ $Eomes^{+}$ among CD8 SP cells as defined in C and D. (**G**) The frequency of Tom^{+} cells within DP, $CD44^{hi}$ $PLZF^{+}$ CD4 and $CD44^{hi}$ $Eomes^{+}$ CD8 gates. Statistical significance was determined by a one-way ANOVA Tukey's (B, E and F) or by Dunnett's multiple comparisons tests (G).

Figure 1

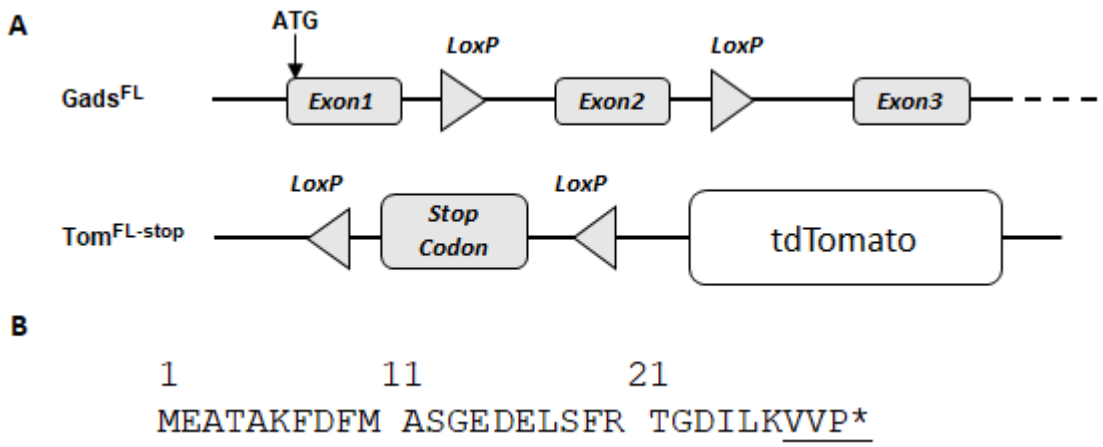
A
ATG
LoxP
LoxP
Gads^FL
Exon1
Exon2
Exon3
LoxP
LoxP
Tom^FL-stop
Stop Codon
tdTomato
B
1 11 21
MEATAKFDFM ASGEDELSFR TGDILKVVP*

Figure 2

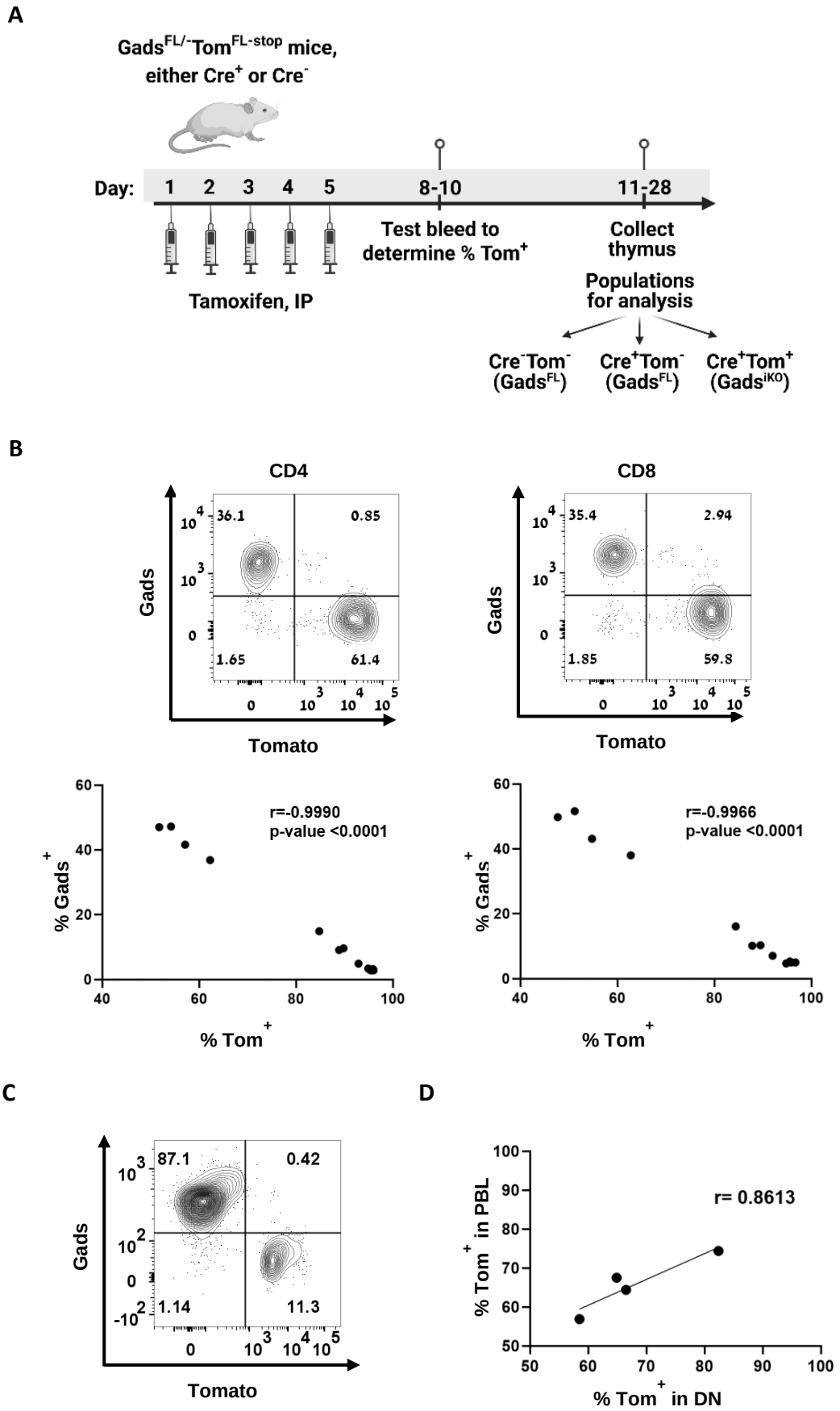
A
Gads$^{FL/-}$Tom$^{FL-stop}$ mice, either Cre$^+$ or Cre$^-$
Day: 1 2 3 4 5 8-10 11-28
Tamoxifen, IP
Test bleed to determine % Tom$^+$
Collect thymus
Populations for analysis
Cre$^-$Tom$^-$ (Gads^{FL})
Cre$^+$Tom$^-$ (Gads^{FL})
Cre$^+$Tom$^+$ (Gads^{iKO})
B
CD4
CD8
Gads
Tomato
36.1
0.85
1.65
61.4
35.4
2.94
1.85
59.8
% Gads$^+$
% Tom$^+$
r=-0.9990
p-value <0.0001
r=-0.9966
p-value <0.0001
C
87.1
0.42
1.14
11.3
D
% Tom$^+$ in PBL
% Tom$^+$ in DN
r= 0.8613

Figure 3

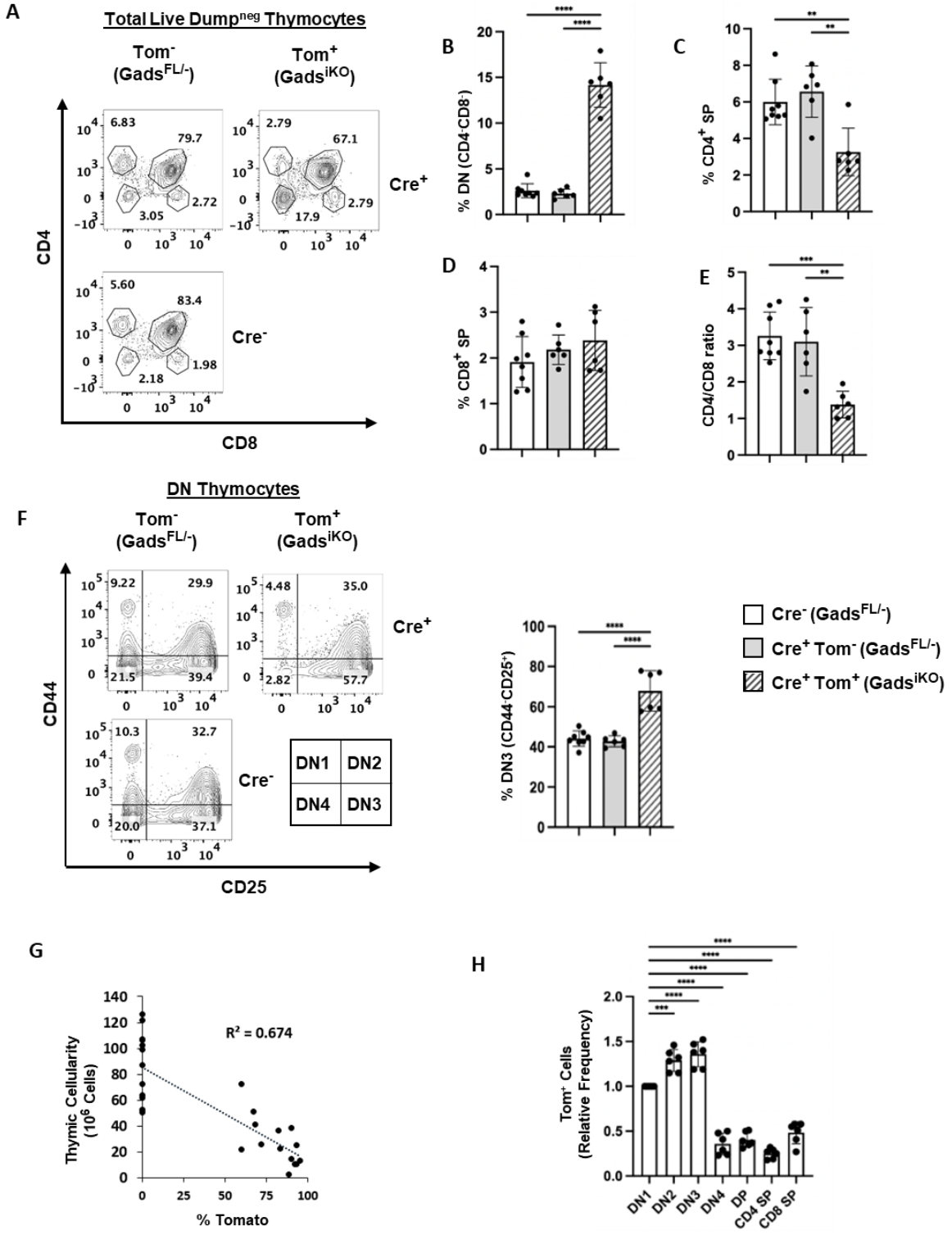
A
Total Live Dump^neg Thymocytes
Tom^- (Gads^FL/-)
Tom^+ (Gads^iKO)
Cre^+
Cre^-
CD4
CD8
B
% DN (CD4^-CD8^-)
C
% CD4^+ SP
D
% CD8^+ SP
E
CD4/CD8 ratio
DN Thymocytes
F
CD44
CD25
DN1
DN2
DN4
DN3
% DN3 (CD44^-CD25^+)
Cre^- (Gads^FL/-)
Cre^+ Tom^- (Gads^FL/-)
Cre^+ Tom^+ (Gads^iKO)
G
Thymic Cellularity (10^6 Cells)
R² = 0.674
% Tomato
H
Tom^+ Cells (Relative Frequency)
DN1
DN2
DN3
DN4
DP
CD4 SP
CD8 SP

Figure 4

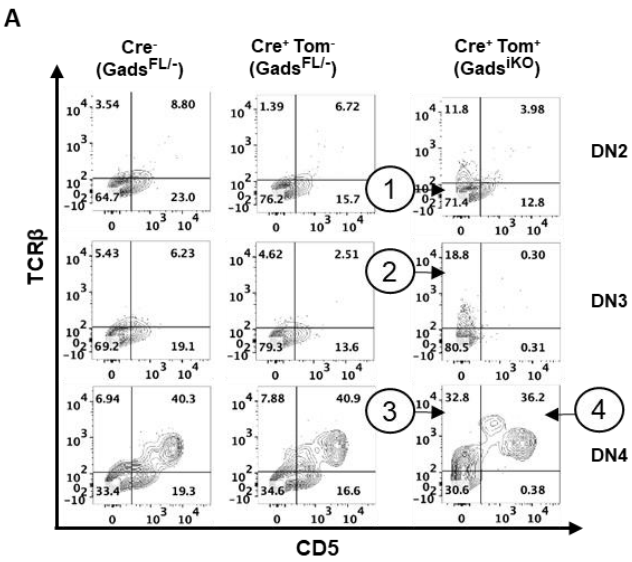

	Population	Definition
1	Early DN	DN2 TCRβ⁻ CD5⁻
2	Arrested β-selection	DN3 TCRβ⁺ CD5⁻
3	Impaired β-selection	DN4 TCRβ⁺ CD5⁻
4	Post-β-selection	DN4 TCRβ⁺ CD5⁺

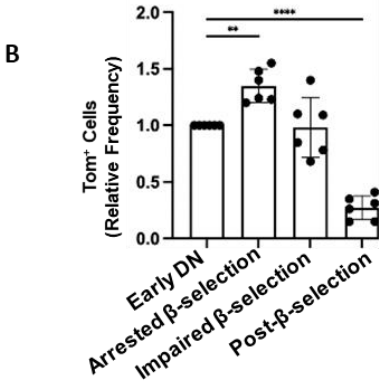

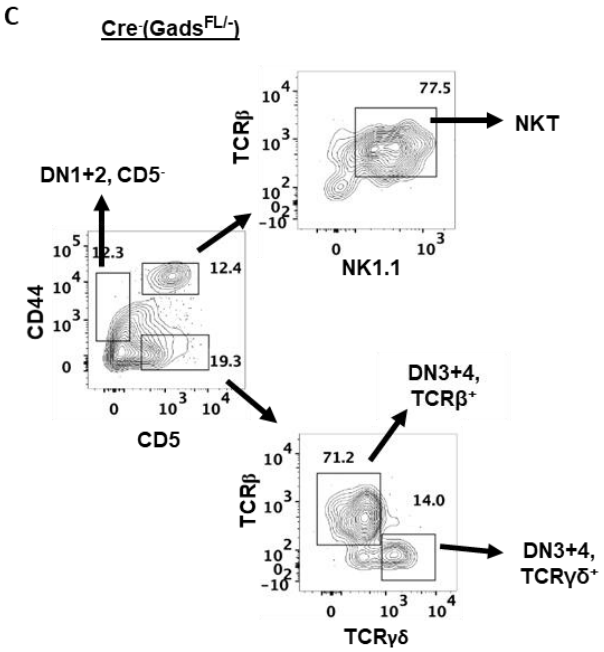

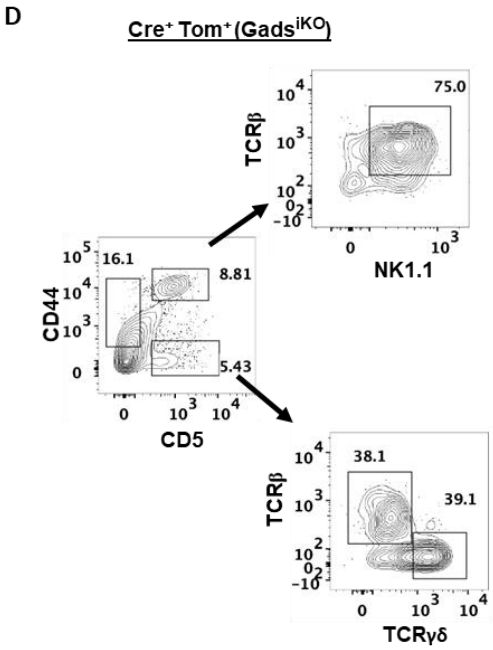

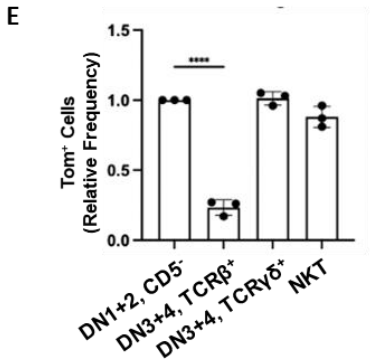

Figure 5

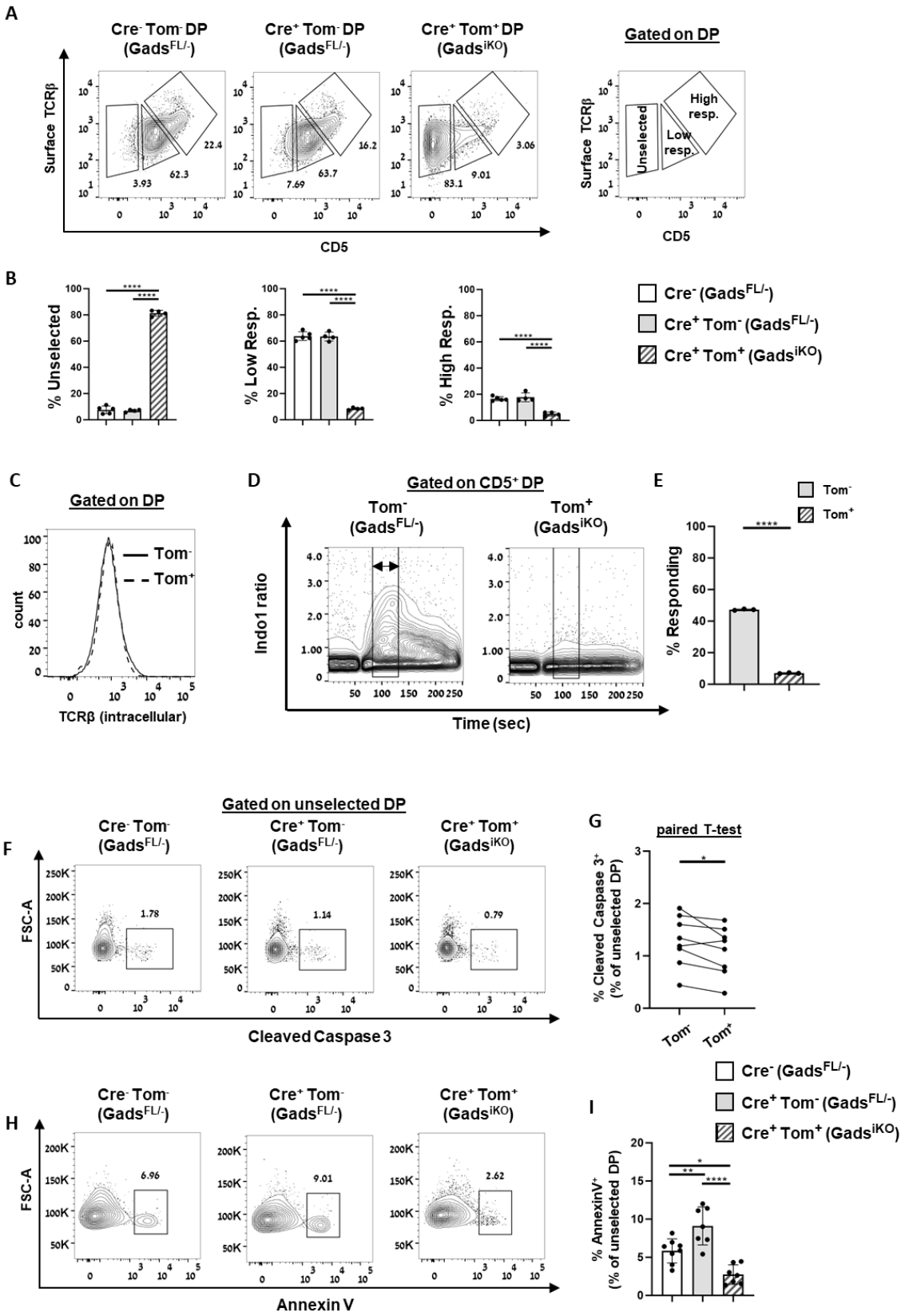
A
Cre- Tom- DP (GadsFL/-)
Cre+ Tom- DP (GadsFL/-)
Cre+ Tom+ DP (GadsiKO)
Gated on DP
Surface TCRβ
CD5
22.4
62.3
3.93
16.2
63.7
7.69
3.06
9.01
83.1
High resp.
Low resp.
Unselected
B
% Unselected
% Low Resp.
% High Resp.
Cre- (GadsFL/-)
Cre+ Tom- (GadsFL/-)
Cre+ Tom+ (GadsiKO)
C
Gated on DP
count
Tom-
Tom+
TCRβ (intracellular)
D
Gated on CD5+ DP
Tom- (GadsFL/-)
Tom+ (GadsiKO)
Indo1 ratio
Time (sec)
E
Tom-
Tom+
% Responding
F
Gated on unselected DP
Cre- Tom- (GadsFL/-)
Cre+ Tom- (GadsFL/-)
Cre+ Tom+ (GadsiKO)
FSC-A
1.78
1.14
0.79
Cleaved Caspase 3
G
paired T-test
% Cleaved Caspase 3+ (% of unselected DP)
Tom-
Tom+
H
Cre- Tom- (GadsFL/-)
Cre+ Tom- (GadsFL/-)
Cre+ Tom+ (GadsiKO)
FSC-A
6.96
9.01
2.62
Annexin V
I
Cre- (GadsFL/-)
Cre+ Tom- (GadsFL/-)
Cre+ Tom+ (GadsiKO)
% AnnexinV+ (% of unselected DP)

Figure 6

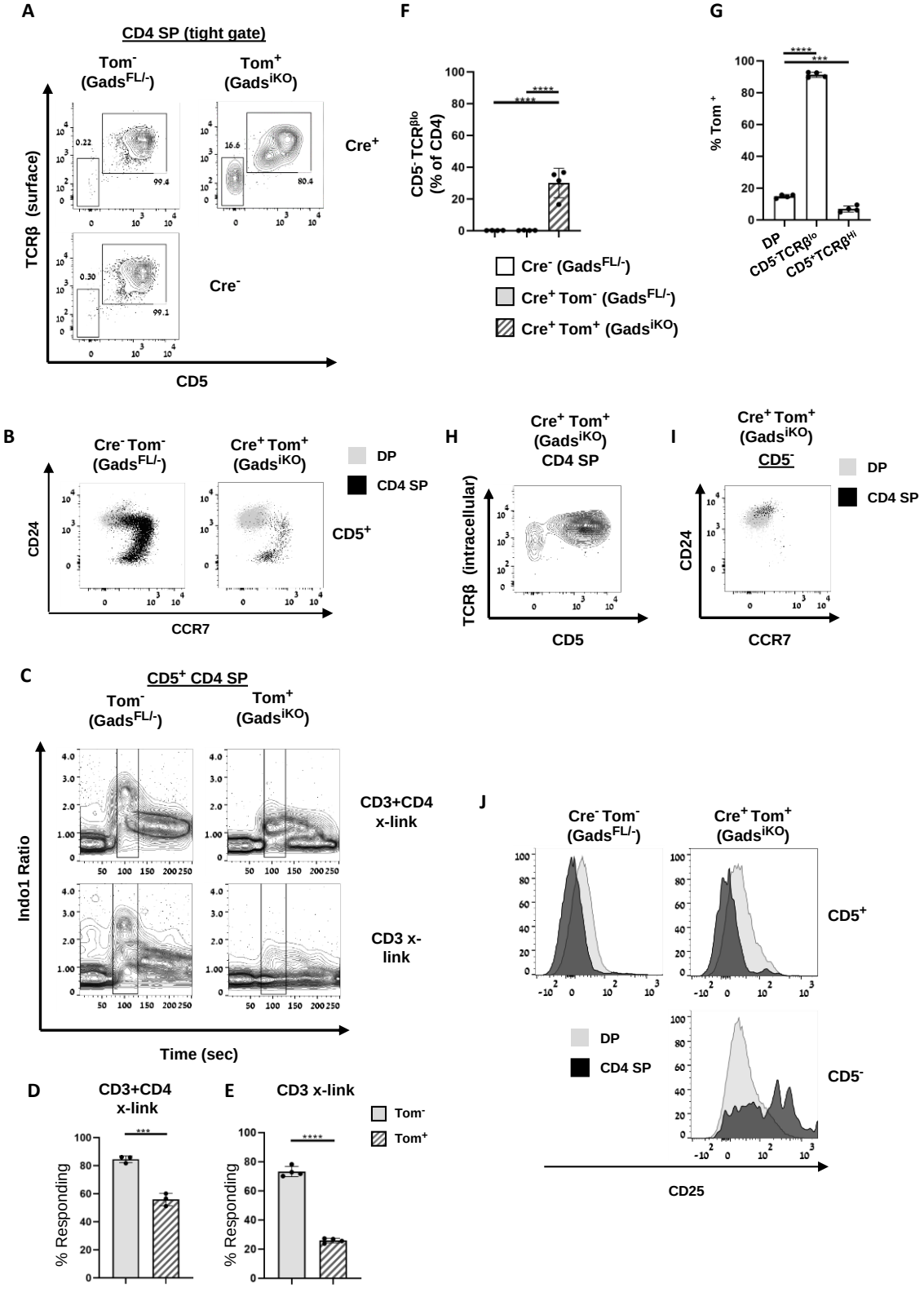
A
CD4 SP (tight gate)
Tom- (GadsFL/-)
Tom+ (GadsiKO)
Cre+
Cre-
TCRβ (surface)
CD5
B
Cre- Tom- (GadsFL/-)
Cre+ Tom+ (GadsiKO)
DP
CD4 SP
CD5+
CD24
CCR7
C
CD5+ CD4 SP
Tom- (GadsFL/-)
Tom+ (GadsiKO)
CD3+CD4 x-link
CD3 x-link
Indo1 Ratio
Time (sec)
D
CD3+CD4 x-link
% Responding
E
CD3 x-link
Tom-
Tom+
F
CD5- TCRβlo (% of CD4)
Cre- (GadsFL/-)
Cre+ Tom- (GadsFL/-)
Cre+ Tom+ (GadsiKO)
G
% Tom+
DP
CD5-TCRβlo
CD5+TCRβHi
H
Cre+ Tom+ (GadsiKO) CD4 SP
TCRβ (intracellular)
CD5
I
Cre+ Tom+ (GadsiKO)
CD5-
DP
CD4 SP
CD24
CCR7
J
Cre- Tom- (GadsFL/-)
Cre+ Tom+ (GadsiKO)
CD5+
CD5-
DP
CD4 SP
CD25

998 **Figure 7**

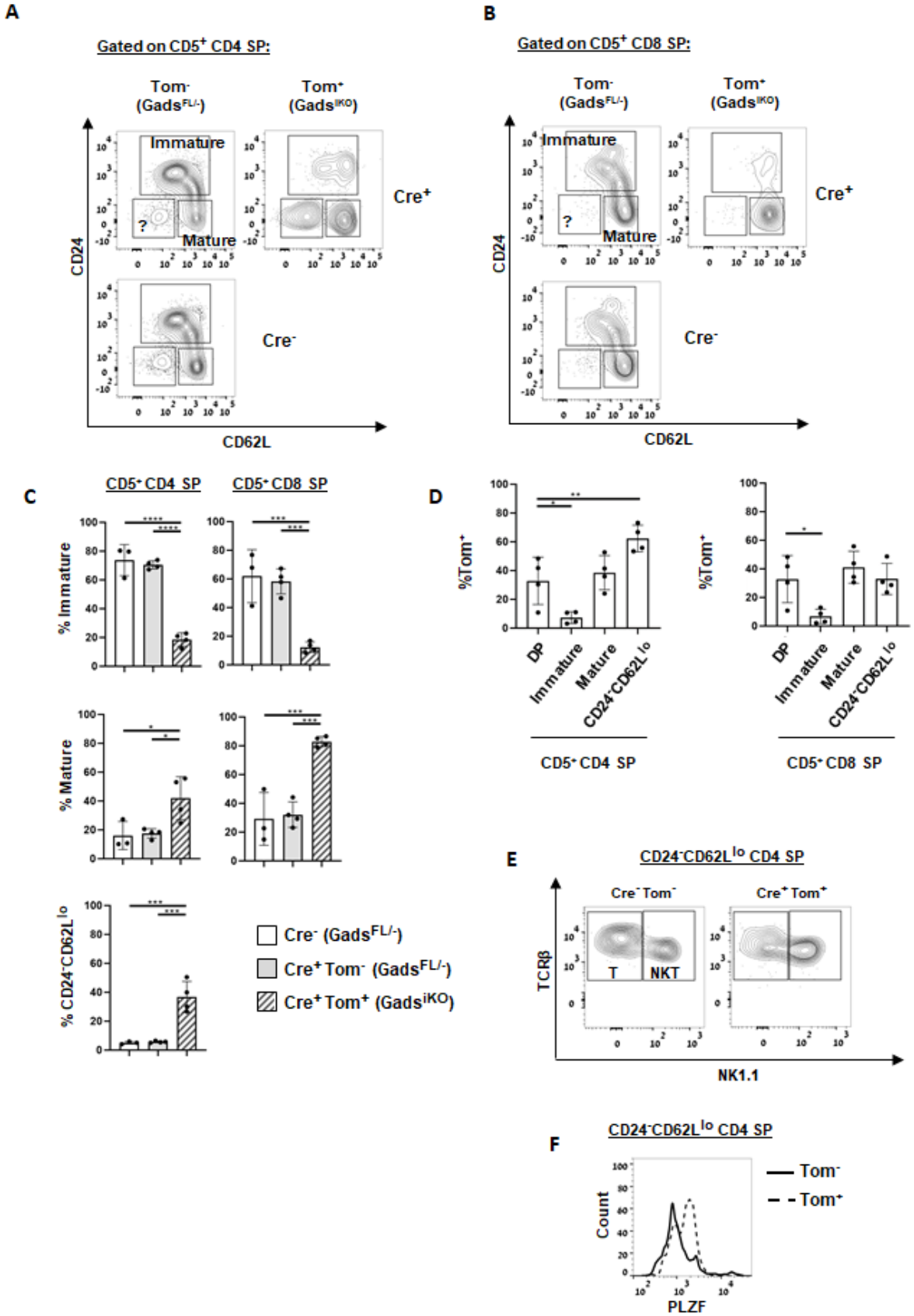

999

1000 **Figure 8**

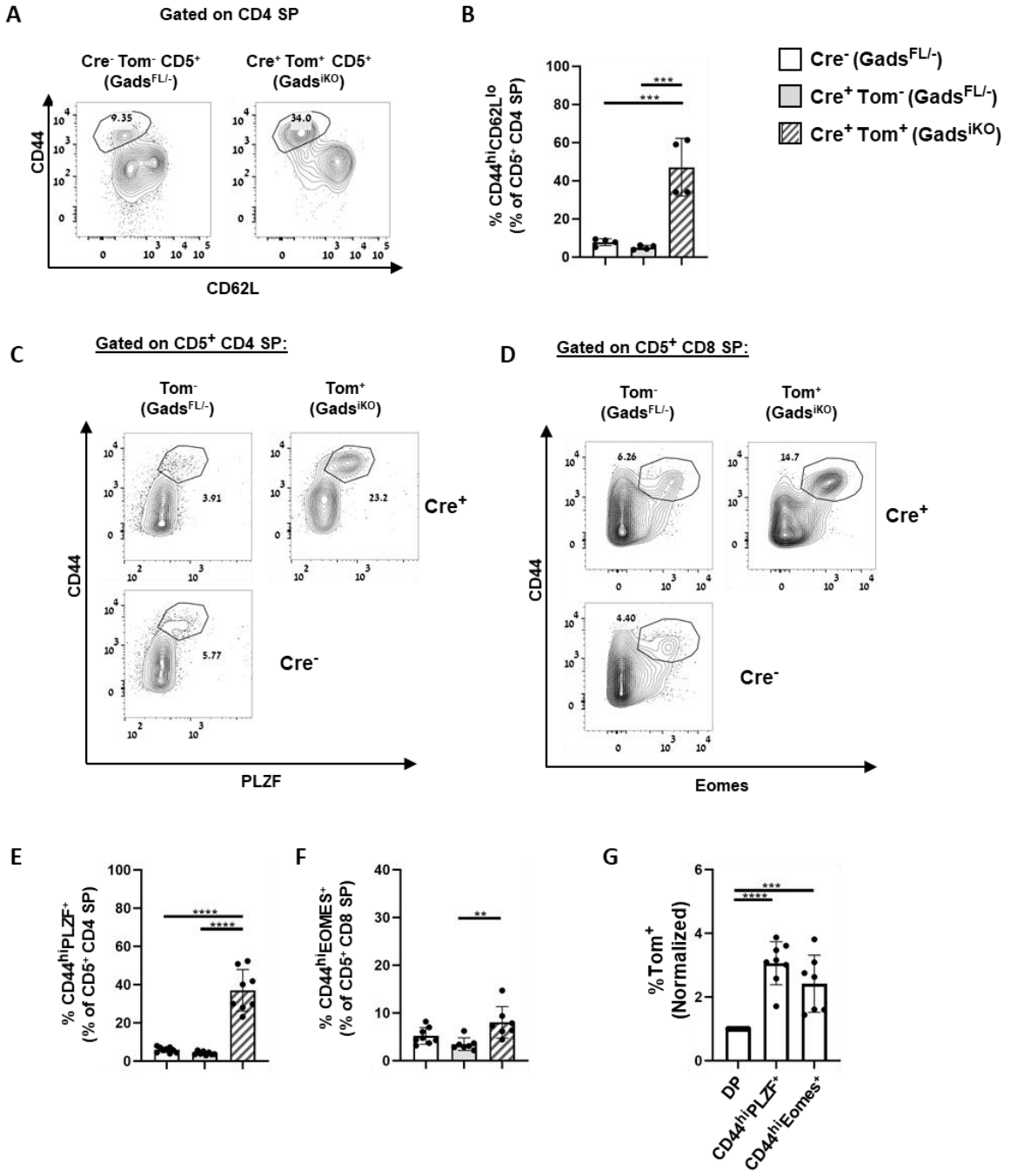

1001